COLUMBIA UNIVERSITY
IN THE CITY OF NEW YORK

JET Collaboration

Consistency of Perfect Fluidity and Jet Quenching in semi-Quark-Gluon Monopole Plasmas

Jiechen Xu
Columbia University

Based on: JX, Jinfeng Liao, Miklos Gyulassy, arXiv:1411.3673
JX, Alessandro Buzzatti, Miklos Gyulassy, JHEP 1408, 063 (2014)

April 10, 2015 @ Baltimore, MD

Outline

- Motivation: inconsistencies between bulk viscous and jet transport properties
- Nonperturbative medium near Tc
- Perturbative jet quenching
- CUJET3.0 = pQCD + semi-QGP + magnetic monopoles
- $\hat{q}/T^3(T)$, $\eta/s(T)$
- Summary

Bulk perfect fluidity vs pQCD jet quenching

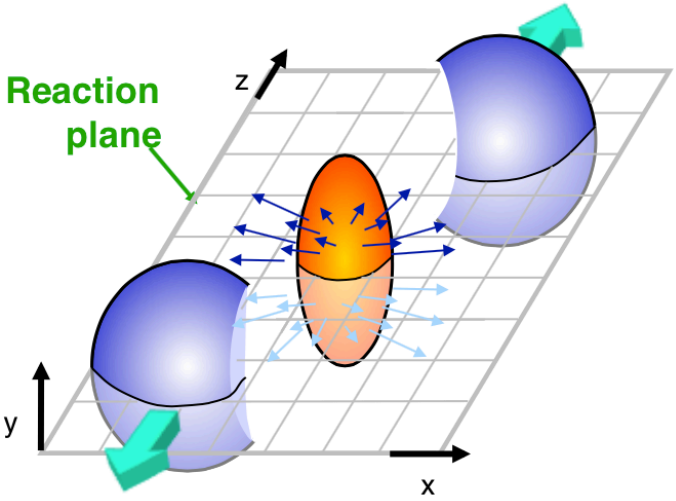

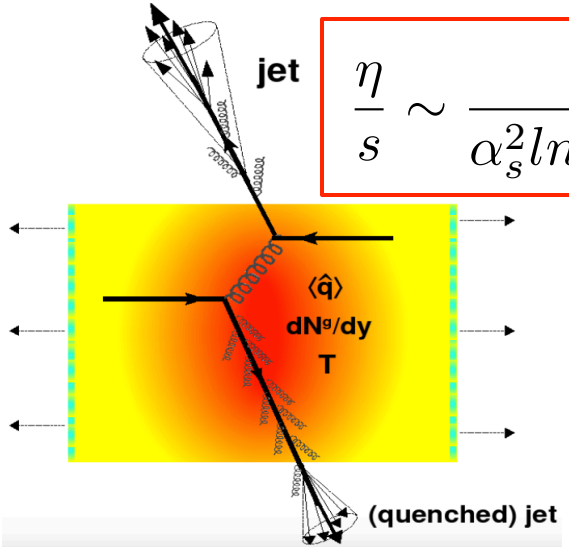

$$\frac{\eta}{s} \sim \frac{1}{\alpha_s^2 ln(\alpha_s^{-1})}$$

Bulk: nonperturbative, η/s~0.1-0.2

Jet quenching: pQCD, η/s~0.5-1.0

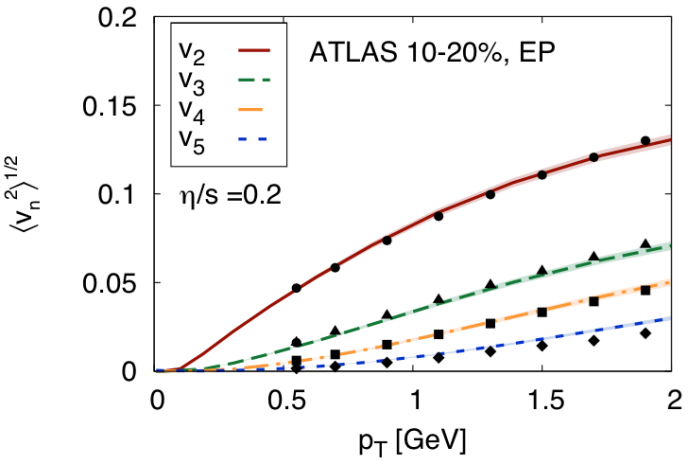

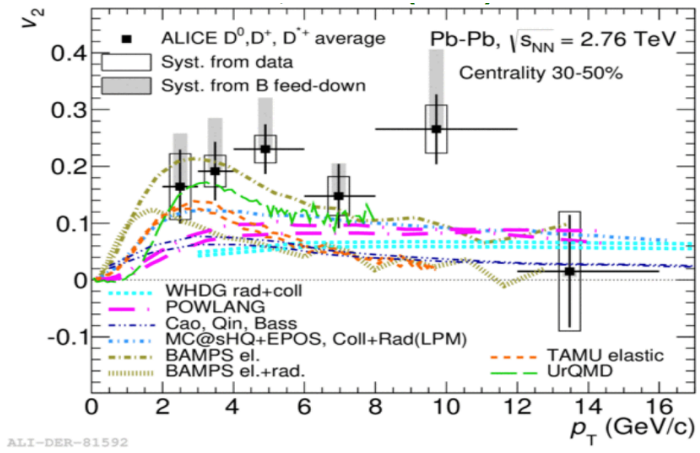

Bulk: IP-Glasma + MUSIC, Gale et al. 2013

Jet quenching: 50% underprediction of high pT v2

❖ Bulk perfect fluidity and jet quenching inconsistent?

Beyond the “standard model” of heavy ion collisions

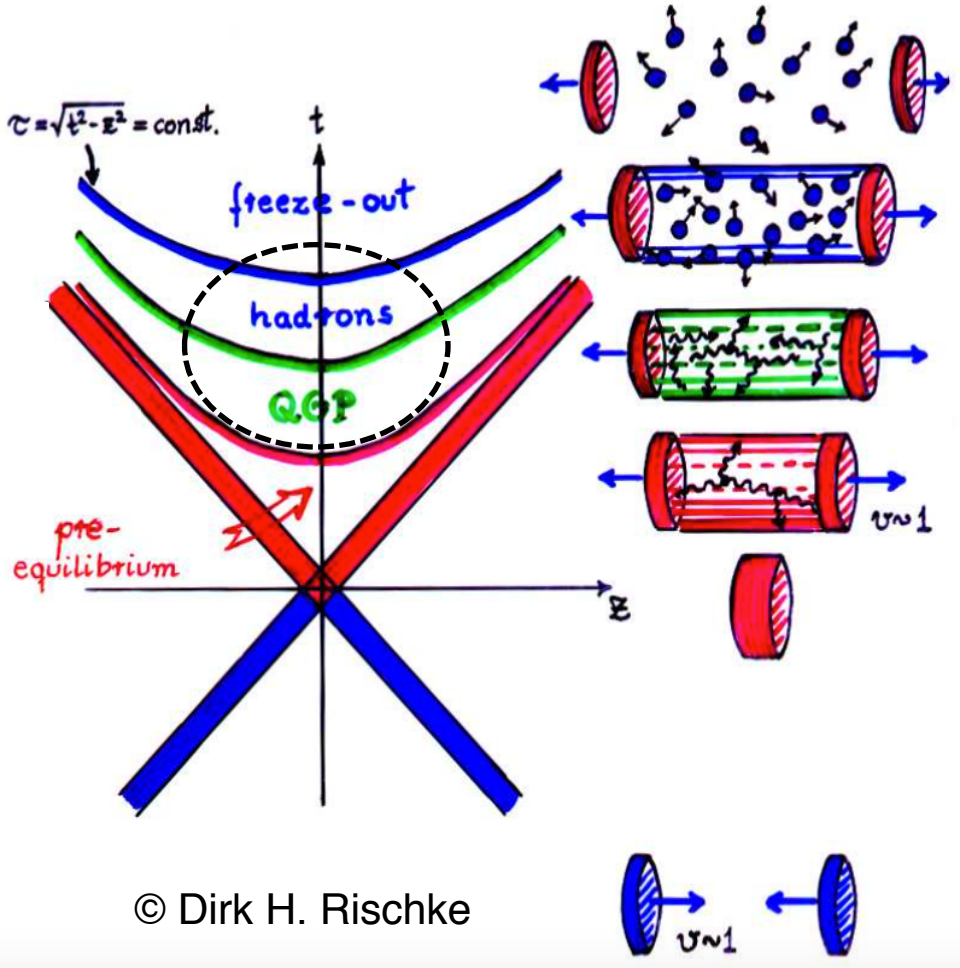

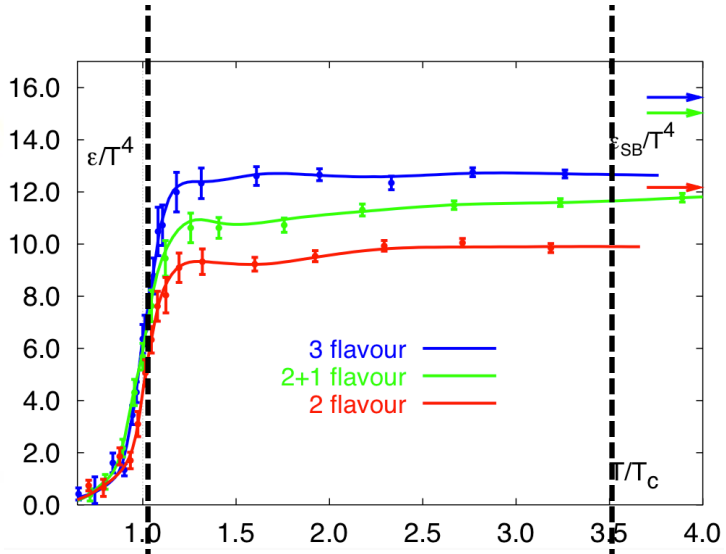

HotQCD Collaboration 2009

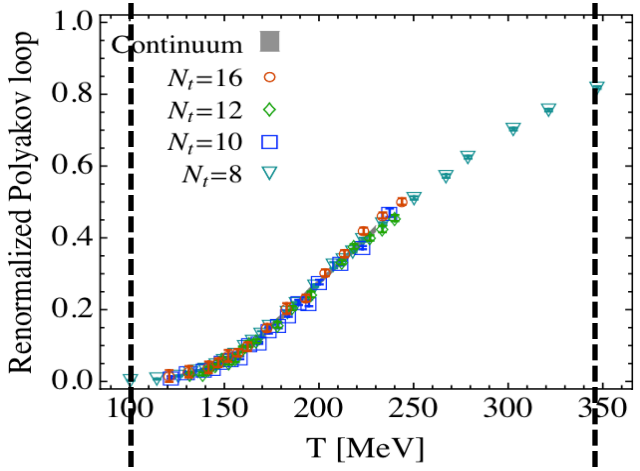

Wuppertal-Budapest 2010

- What would be a lattice compatible, microscopic description of the near Tc matter?
  - Does this help reconciling the “soft” vs “hard” transport inconsistency?

Liao-Shuryak "E-M See-Saw" Scenario

T<< Lambda_QCD | T ~ Lambda_QCD | T>> Lambda_QCD

Vacuum: confined — Tc — sQGP — ***wQGP: screening*** — T

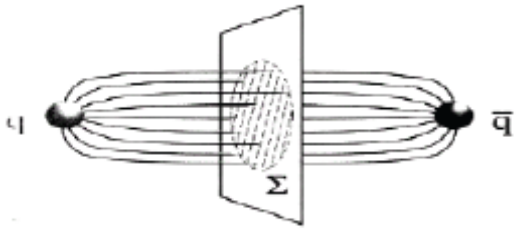

Emergent plasma with E & M charges:
chromo-magnetic monopoles are the "missing DoF"

Plasma of E-charges
E-screening: g T
M-screening: g^2 T

Electric Flux Tube:
Magnetic Condensate

$$\alpha_E * \alpha_M = 1.$$

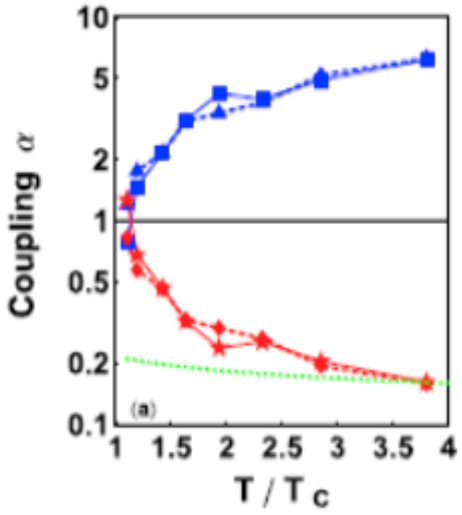

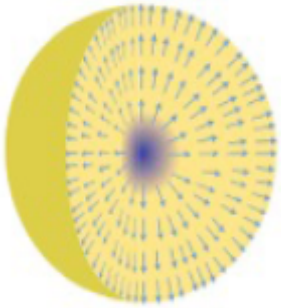

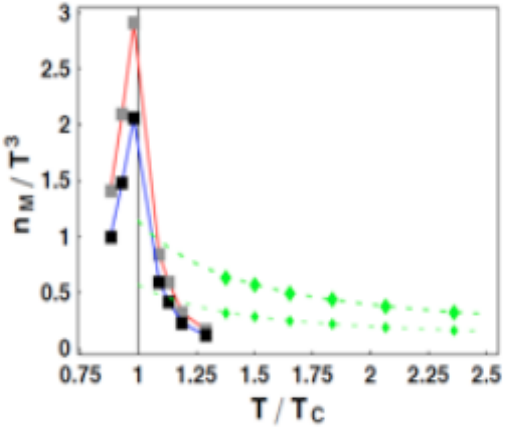

Phys.Rev.C75:054907,2007; Phys.Rev.Lett.101:162302,2008; Phys.Rev.C77:064905,2008; Phys.Rev.D82:094007,2010; Phys.Rev.Lett.109:152001,2012.

❖ Jinfeng Liao, APS DNP Hawaii 2014

The QCD matter near Tc

- Near Tc: semi-QGP + magnetic monopoles (sQGMP)?

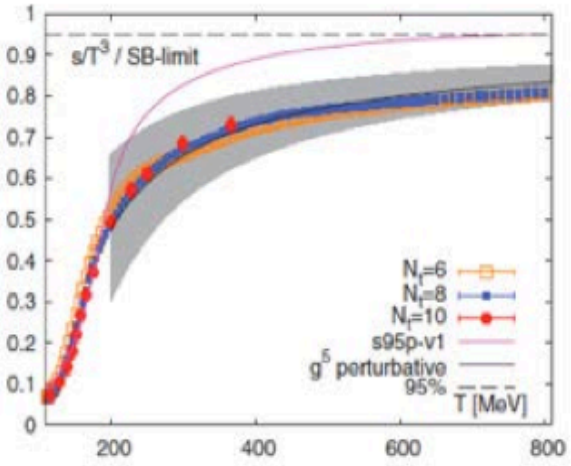

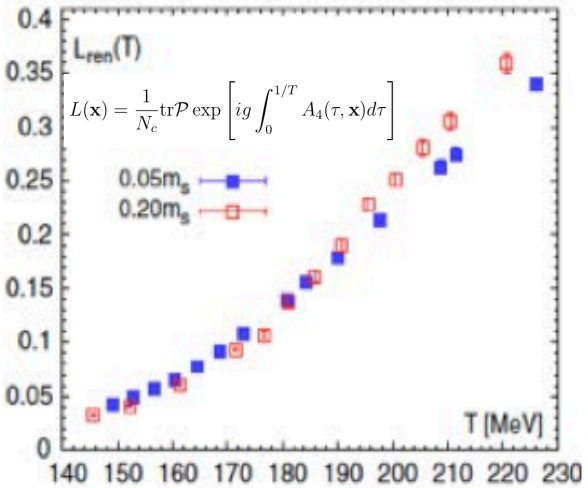

A region around Tc with liberated degrees of freedom

but only partially liberated color-electric objects—missing D.o.F.:

semi-QGP + emergent magnetic component

- Courtesy of Jinfeng Liao

- How can we implement such a microscopic model of QGP in the strong coupling regime into a pQCD jet energy loss framework?
  - Does this explain all the jet quenching data at RHIC and LHC?
  - Does this provide a quantitative connenction between the perfect fluidity of QGP and pQCD jet quenching?

pQCD jet quenching

- pQCD jet energy loss models: AMY, ASW, BDMPS-Z, Higher twist, (D)GLV…

- (D)GLV
  - The plasma: well-separated, static, color screened scattering centers
  - Energy loss: expansion in the number of parton-medium scatterings (opacity expansion)
    - Dominated by the first hard contribution. (“Thin plasma”)
  - Include interference of “vacuum” radiation, vertex radiation and gluon rescatterings

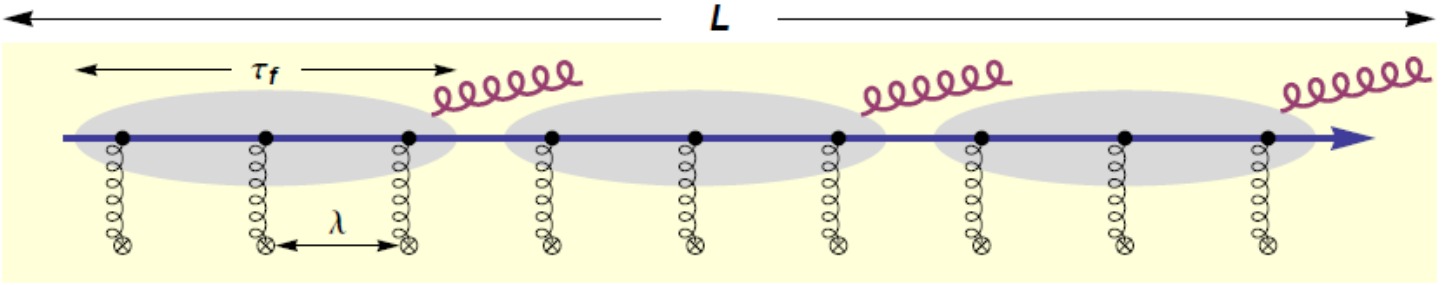

- $\tau_f<\lambda<L$ Incoherent multiple collisions
- $\lambda<\tau_f<L$ LPM effect
- $\lambda<L<\tau_f$ “Factorization” limit

The heavy quark energy loss puzzle & The surprising transparency of QGP at LHC

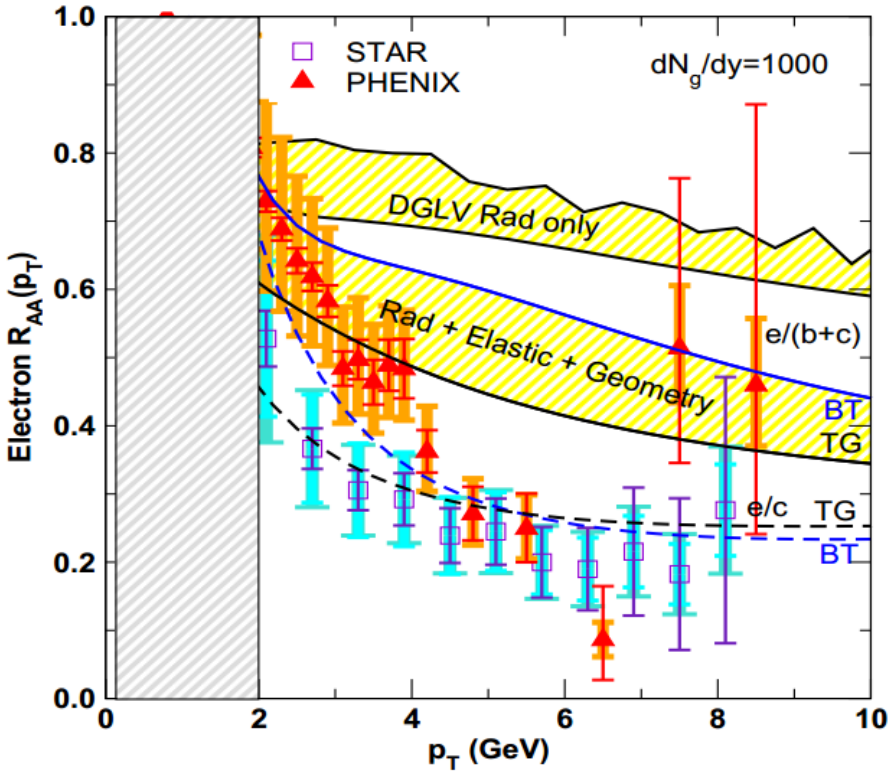

WHDG, NPA784,426(2007)

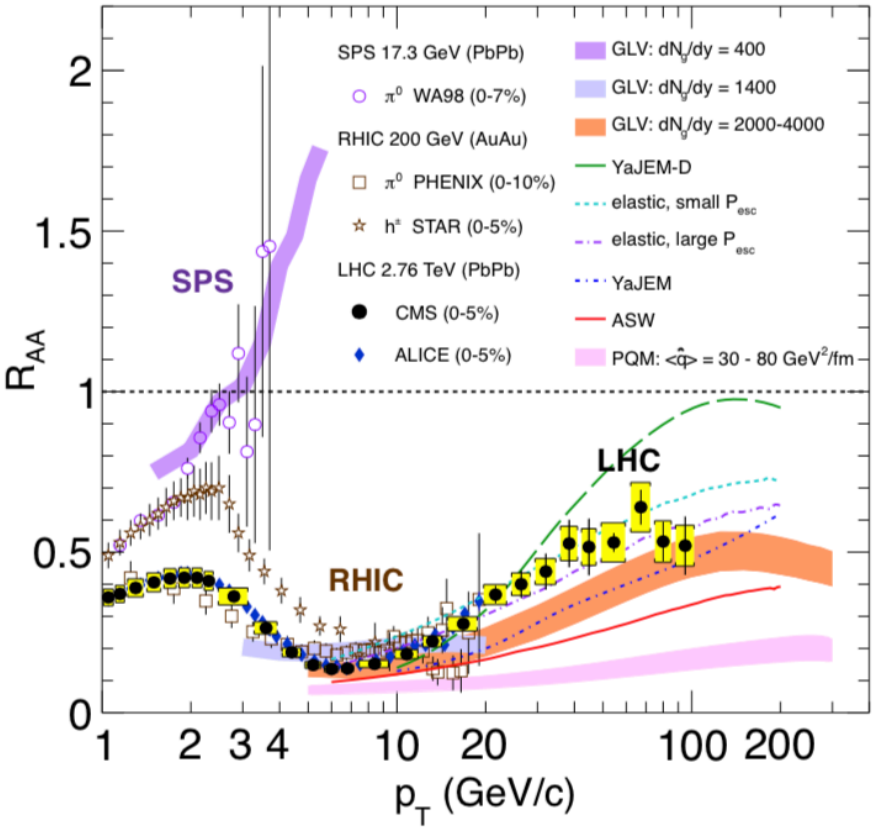

CMS-HIN-10-005

- "Heavy Quark Energy Loss Puzzle"
  - Scattering centers recoil?
  - Realistic path length fluctuations?
- "The surprising transparency of QGP at LHC"
  - The opacity's dependence on density is weaker than linear
  - Smaller coupling at LHC?

CUJET: to solve the heavy quark energy loss puzzle + to explain the surprising transparency of QGP at LHC

❖ Recoiling scattering centers

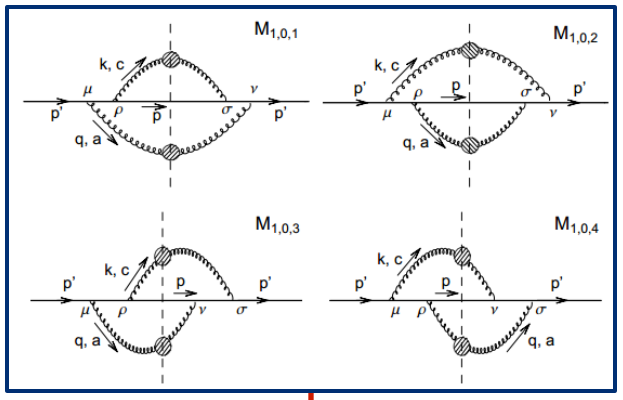

$$\lambda_{\rm dyn} \Longleftrightarrow \lambda_{\rm stat} = \frac{\lambda_{\rm dyn}}{c(n_f)}$$

$$\left[\frac{\mu^2}{\boldsymbol{q}^2(\boldsymbol{q}^2+\mu^2)}\right]_{\rm dyn} \Longleftrightarrow \left[\frac{\mu^2}{(\boldsymbol{q}^2+\mu^2)^2}\right]_{\rm stat}$$

Djordjevic and Heinz, PRC (2008)

❖ Path length fluctuations: $T(\tau_{max}) = T_f$

❖ Multi-scale running strong coupling

$$Q^2 = \mathbf{q}^2$$

$$Q_2^2 = q^2 - M^2 = \frac{\mathbf{k}^2}{x_+(1-x_+)} + \frac{x_+ M^2}{1-x_+} + \frac{m_g^2}{x_+}$$

$$Q^2 = (2T)^2$$

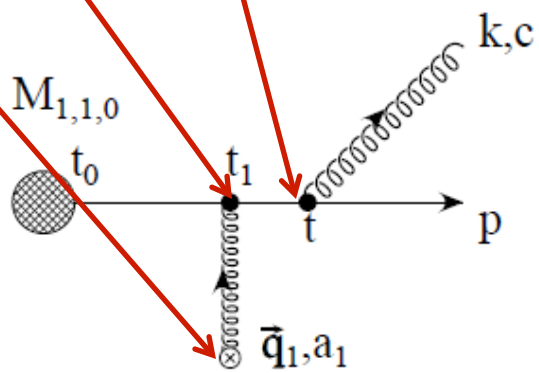

Buzzatti, Gyulassy, 2013; JX, Buzzatti, Gyulassy, 2014

❖ Elastic: S. Peigne and A. Peshier, PRD 77, 114017 (2008)

$$\alpha_s^2 \log\frac{4ET}{\mu^2} \longrightarrow \alpha_s(\mu^2)\alpha_s(4ET)\log\frac{4ET}{\mu^2(\alpha_s(4T^2);T)}$$

CUJET2.0: [pQCD+HTL+Elastic] + [2+1D Viscous Hydro]

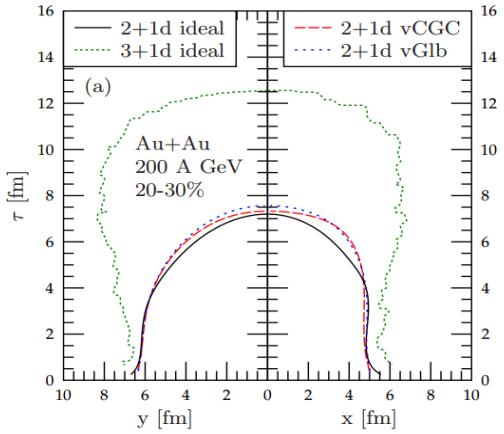

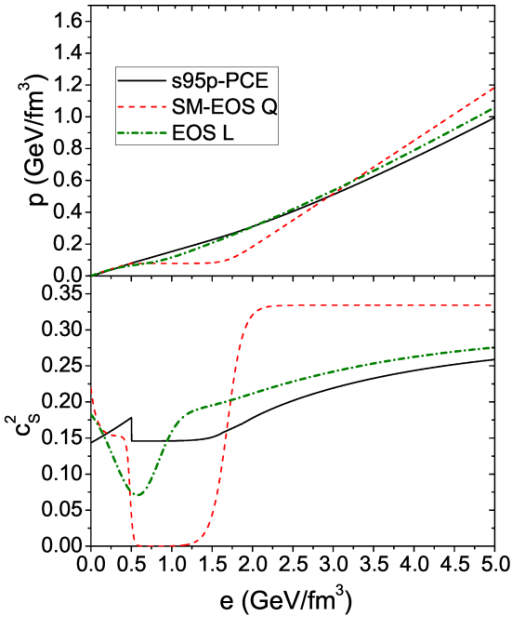

T. Renk, H. Holopainen, U. Heinz and C. Shen, PRC 83, 014910 (2011)
C. Shen, U. Heinz, P. Huovinen and H. Song, PRC 82, 054904 (2010)
H. Song and U. Heinz, PRC 78, 024902 (2008)

- Couple running coupling DGLV opacity series to VISH2+1 transversely expanding QGP fluid fields (T(x,t),v(x,t))
- RHIC Au+Au 200AGeV & LHC Pb+Pb 2.76ATeV
  - Equaiton of State: s95p-v0-PCE
  - Initial Condition: MC-Glauber
  - η/s=0.08
  - Initial Time: 0.6fm/c
  - Cooper-Frye freeze-out temperature: 120MeV
- Viscous hydro backgrounds compatible with measurements of low pT particle production spectra and flow harmonics

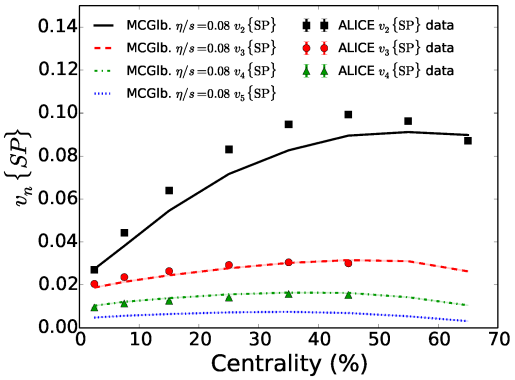

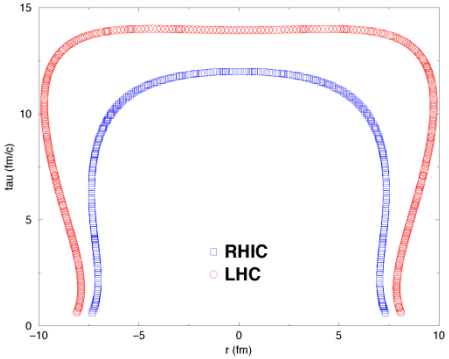

Courtesy of Chun Shen

CUJET2.0: light hadron and open heavy flavor R_{AA}

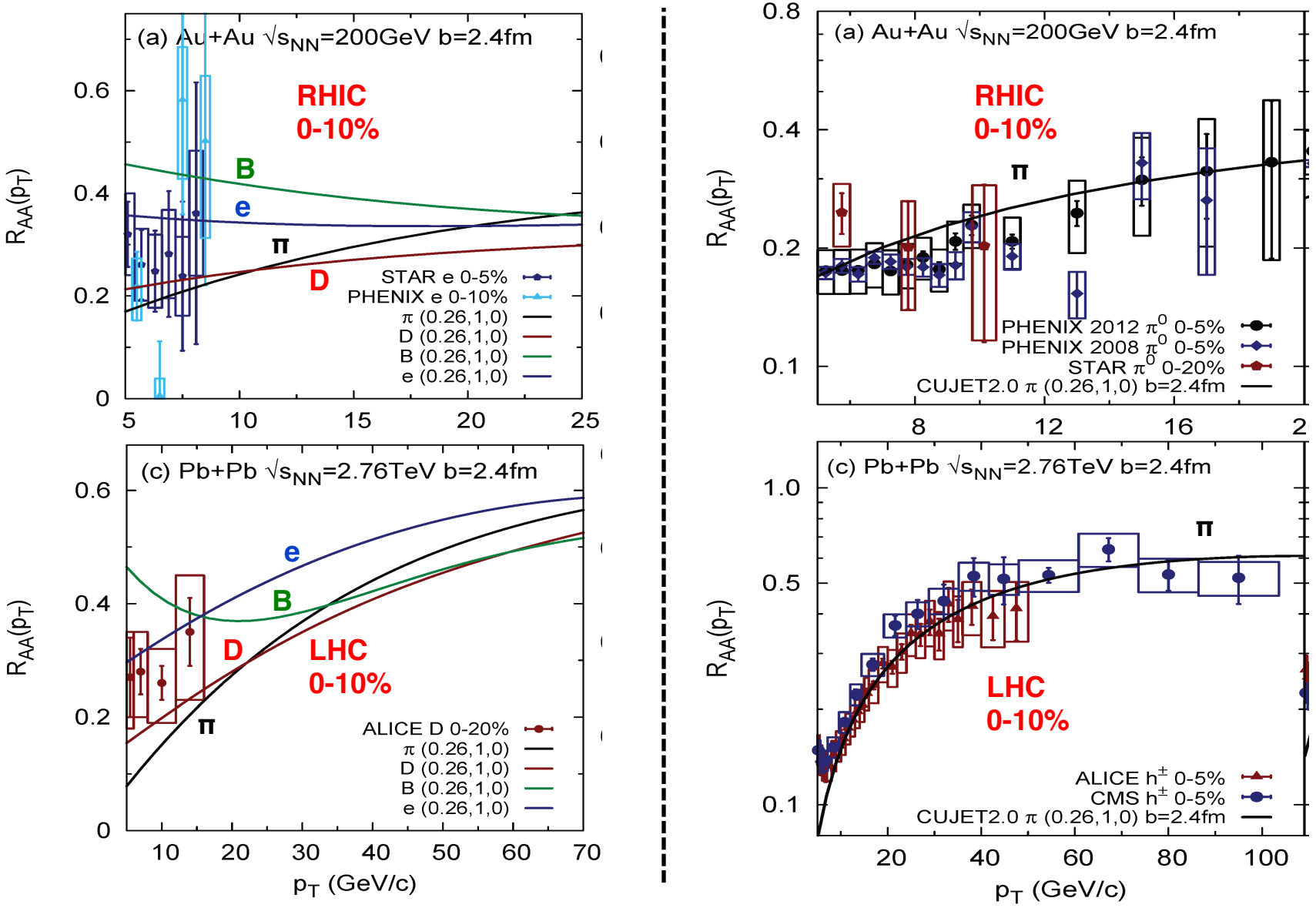

JX, A. Buzzatti, M. Gyulassy, JHEP 1408, 063 (2014)

Jet quenching parameter (qhat) and η/s

$$\hat{q} = \rho \int d^2q_\perp q_\perp^2 \frac{d\sigma}{d^2q_\perp}$$

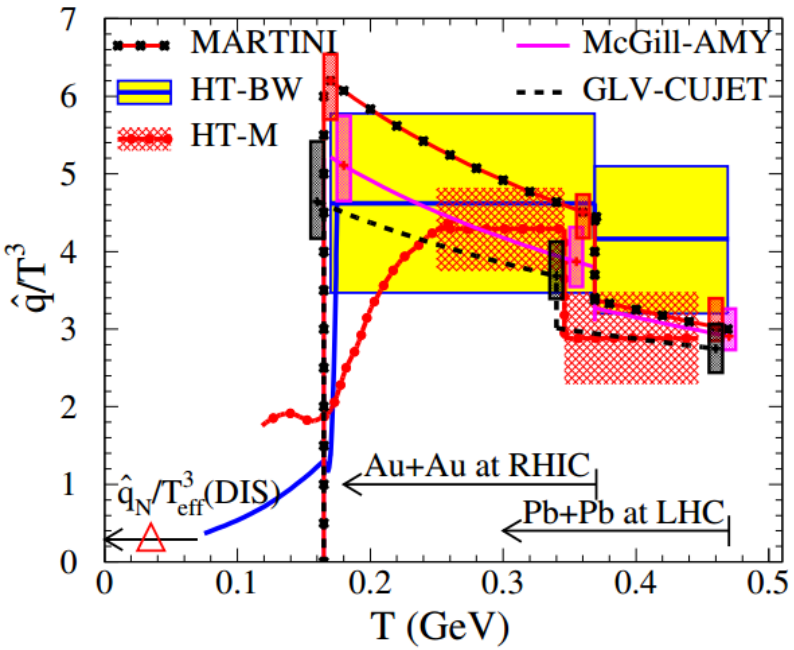

JET Collaboration, PRC 90, 014909 (2014)

$$\frac{\hat{q}}{T^3} \approx \begin{cases} 4.6 \pm 1.2 & \text{at RHIC,} \\ 3.7 \pm 1.4 & \text{at LHC,} \end{cases}$$

$$\hat{q} \approx \begin{cases} 1.2 \pm 0.3 \\ 1.9 \pm 0.7 \end{cases} \text{GeV}^2/\text{fm at} \quad \begin{matrix} T = 370 \text{ MeV}, \\ T = 470 \text{ MeV}, \end{matrix}$$

- Kinetic theory estimate of η/s from qhat

$$\eta/s = \frac{1}{s}\frac{4}{15}\sum_a \rho_a \langle p \rangle_a \lambda_a^{tr}$$

$$= \frac{4T}{5s}\sum_a \rho_a \left(\sum_b \rho_b \int_0^{\langle \mathcal{S}_{ab} \rangle/2} dq^2 \frac{4q^2}{\langle \mathcal{S}_{ab} \rangle} \frac{d\sigma_{ab}}{dq^2} \right)^{-1}$$

$$= \frac{18T^3}{5s}\sum_a \rho_a / \hat{q}_a(T, E = 3T) \quad , \qquad (1$$

Danielewicz, Gyulassy, PRD 1985

$$\frac{\eta}{s} \begin{cases} \approx \\ \gg \end{cases} 1.25 \frac{T^3}{\hat{q}} \begin{cases} \text{for weak coupling,} \\ \text{for strong coupling.} \end{cases}$$

Majumder, Muller, Wang, PRL 2007

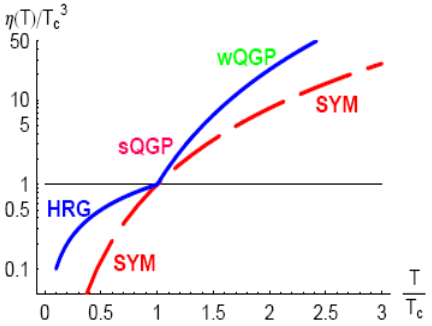

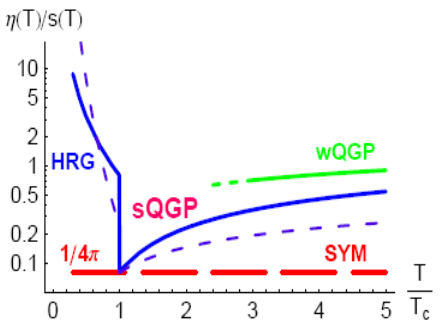

Hirano, Gyulassy, NPA 2006

Jet-medium coupling: from transparency to opaqueness

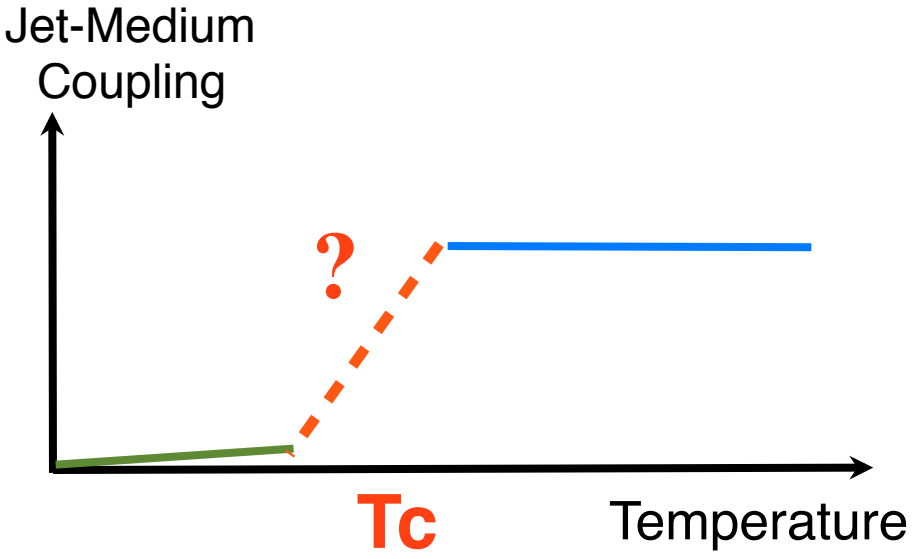

"Waterfall" scenario

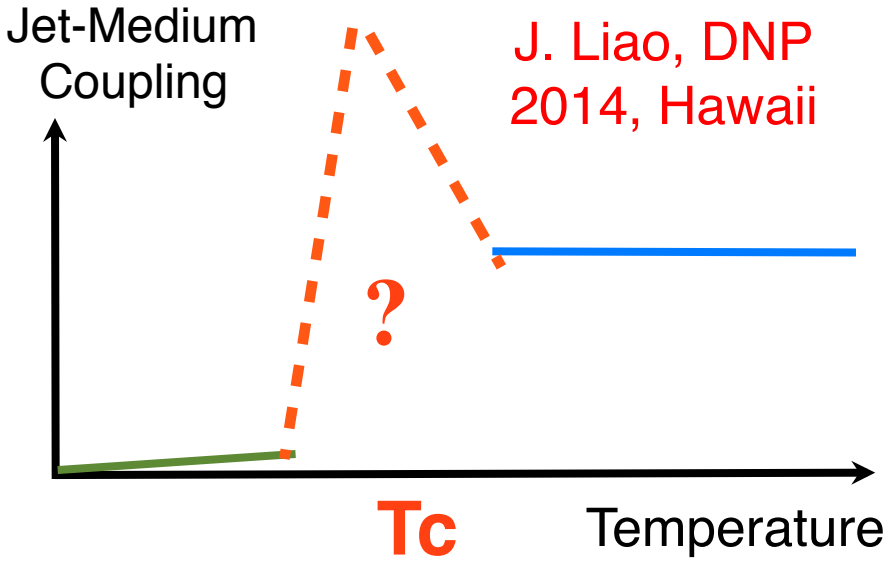

"Volcano" scenario

- How does jet opacity for T>>Tc connect to jet transparency for T<<Tc?
- Is this scenario compatible with the perfect fluidity of QGP near Tc?
- How to systematically implement the microscopic sQGMP model into a jet quenching framework?

CUJET3.0 = pQCD + semi-QGP + mag. monopoles

We now include both color-electric and color-magnetic scattering centers.

Original DGLV has only quark/gluon scattering centers

$$\frac{dE}{dx} \propto \ldots \int_{q^2} \left[\frac{n_e \left(\alpha_s(q^2)\alpha_s(q^2)\right) f_E^2}{q^2(q^2+f_E^2\mu^2)} + \frac{n_m \left(\alpha_s^e(q^2)\alpha^m(q^2)\right) f_M^2}{q^2(q^2+f_M^2\mu^2)} \right] \ldots$$

$$\frac{dE}{dx} \propto \ldots \int_{q^2} \frac{n_e\, \alpha_s^2(q^2)\, f_E^2}{q^2(q^2+f_E^2\mu^2)} \ldots$$

$$\frac{dE}{dx} \propto \ldots \int_{q^2} \frac{n_T}{(q^2+f_E^2\mu^2)(q^2+f_M^2\mu^2)} \times \kappa(q^2,T)$$

=1, by Dirac Quantization

$$\kappa(q^2,T) \equiv \alpha_s^2(q^2)\chi_T \left(f_E^2 + \frac{f_E^2 f_M^2 \mu^2}{q^2}\right) + (1-\chi_T)\left(f_M^2 + \frac{f_E^2 f_M^2 \mu^2}{q^2}\right)$$

$$\chi_T = c_q L + c_g L^2$$

Polyakov Loop suppressed color electric component

$$f_E = \sqrt{\chi_T}$$

$$f_M = C_m g_T$$

$$L(\mathbf{x}) = \frac{1}{N_c} \mathrm{tr} \mathcal{P} \exp\left[ig \int_0^{1/T} A_4(\tau,\mathbf{x}) d\tau\right]$$

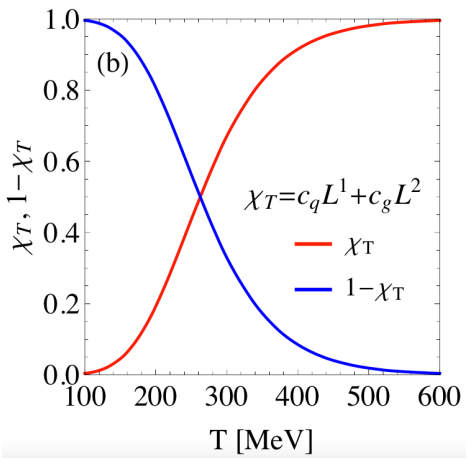

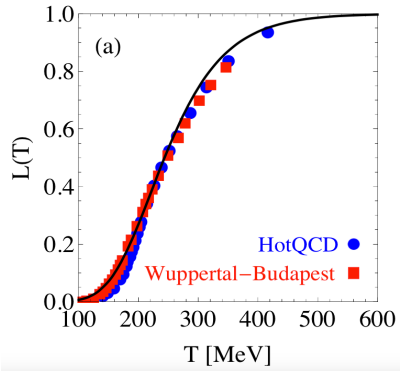

Bazavov et al., PRD 80 (2009)
Borsanyi et al., JHEP 09 (2010)

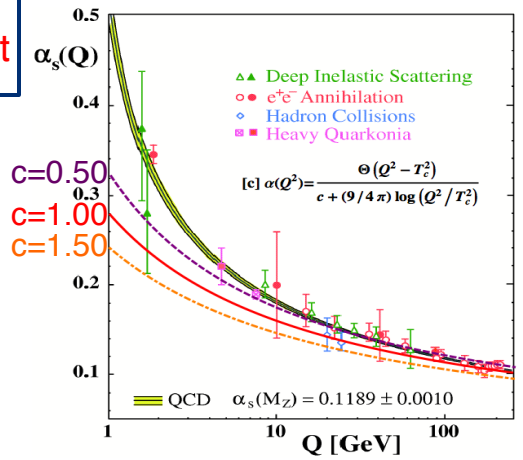

$$\alpha_s^2(q^2) \approx [1/[c + (9/2\pi)Log(q/\Lambda)]]^2$$

Lattice Constraints: Polyakov Loop, EOS, Screening Masses

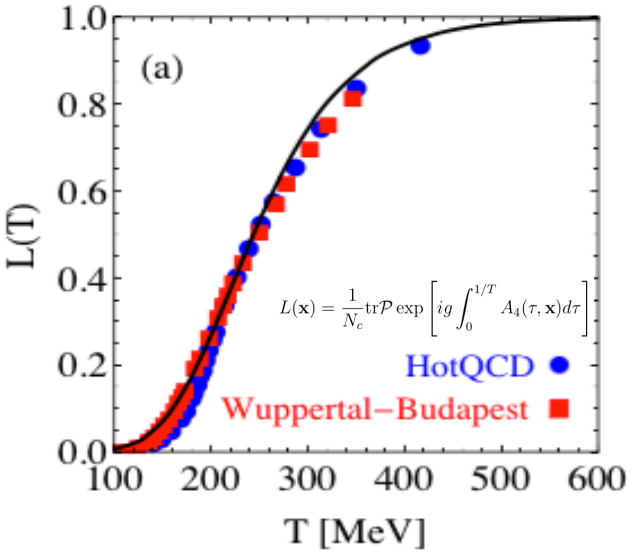

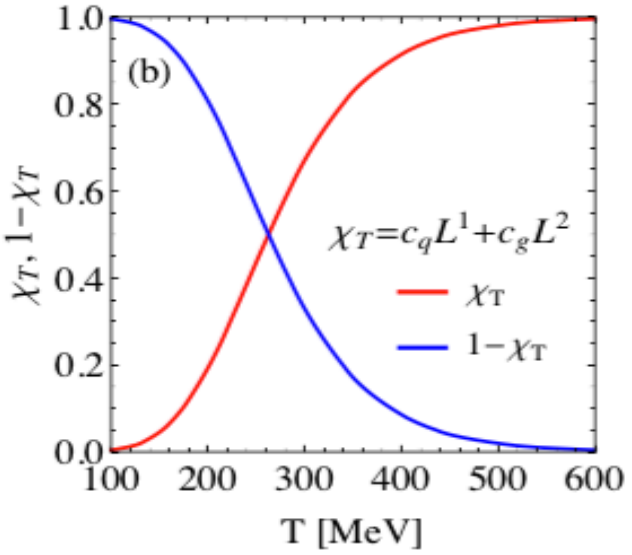

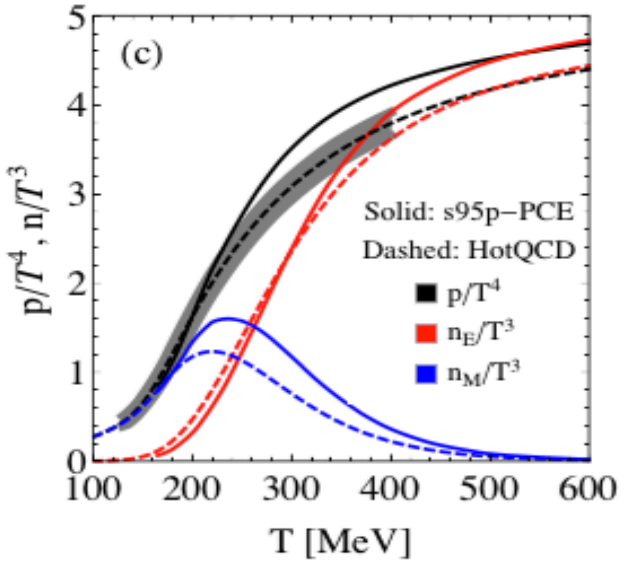

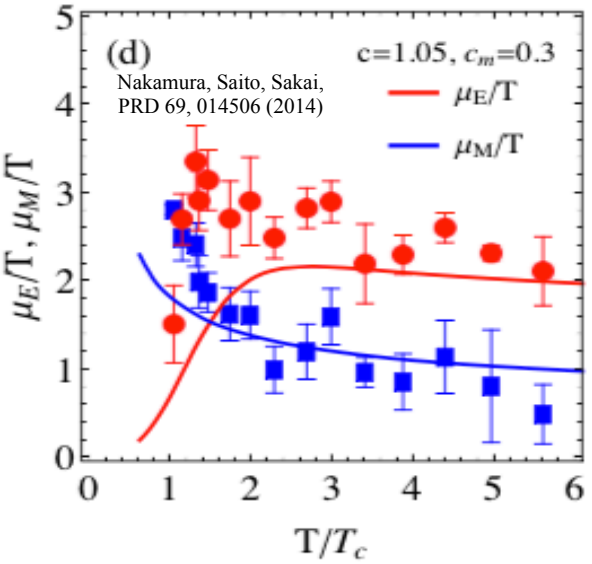

- The CUJET3.0 implementations of electric and magnetic components are well constrained by available lattice data. The only adjustable parameter in this model is “c”.

CUJET3.0 simultaneously describes high pT (R_{AA}+v_2)*(light + heavy)*(RHIC+LHC)

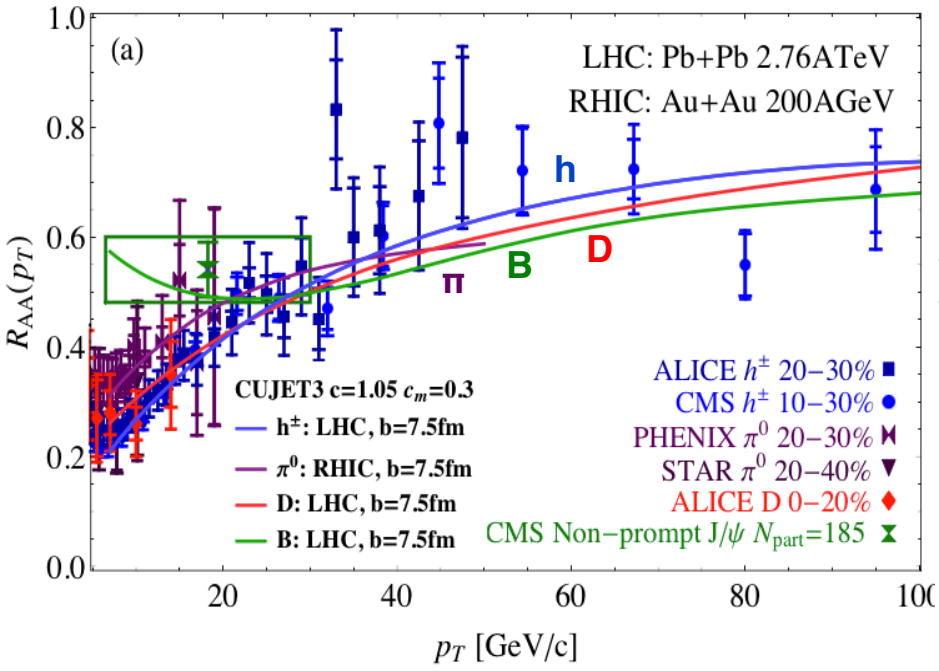

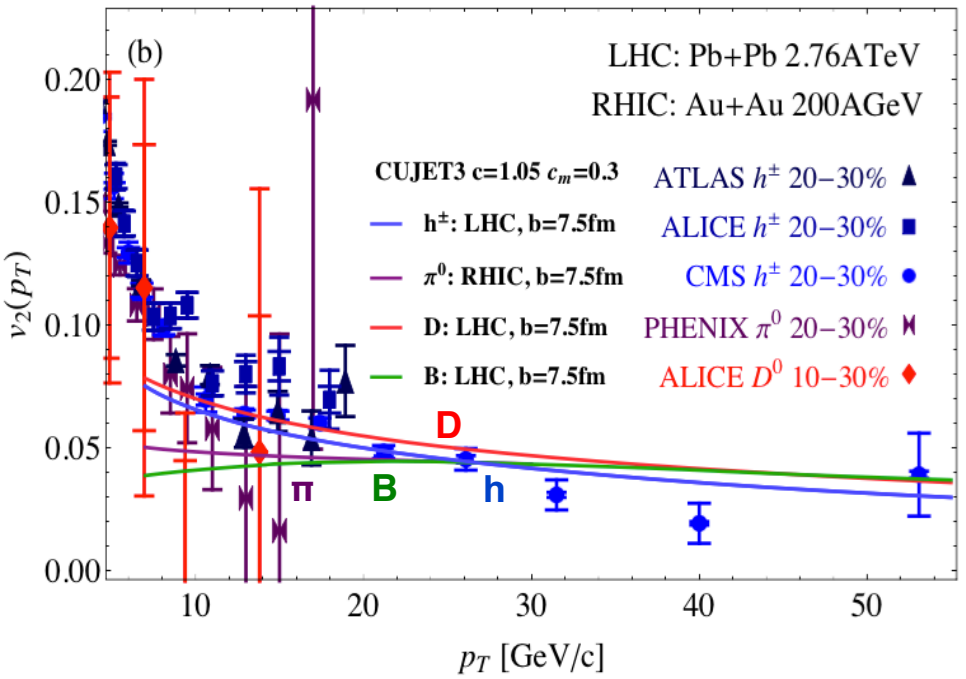

JX, J. Liao, M. Gyulassy, arXiv:1411.3673

The combined set of observables

(R_{AA}+V_2)*(RHIC+LHC)*(pion+D+B)

are consistently accounted for (within present experimental errors) in the CUJET3.0 framework using lattice data constrained sQGMP near Tc + pQCD jet quenching kernal

Open charm's and beauty's high p_T R_{AA} and v_2 at RHIC and LHC (20-30% centrality) from CUJET3.0

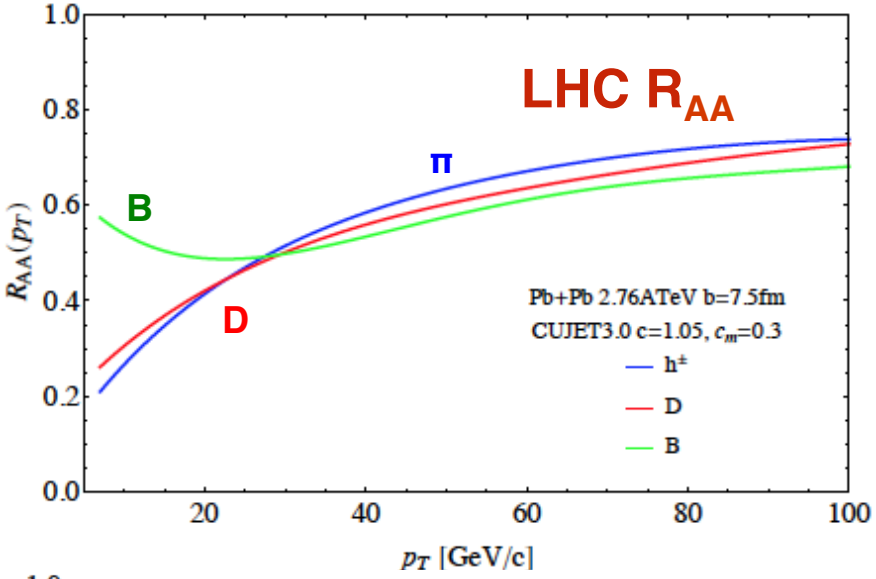

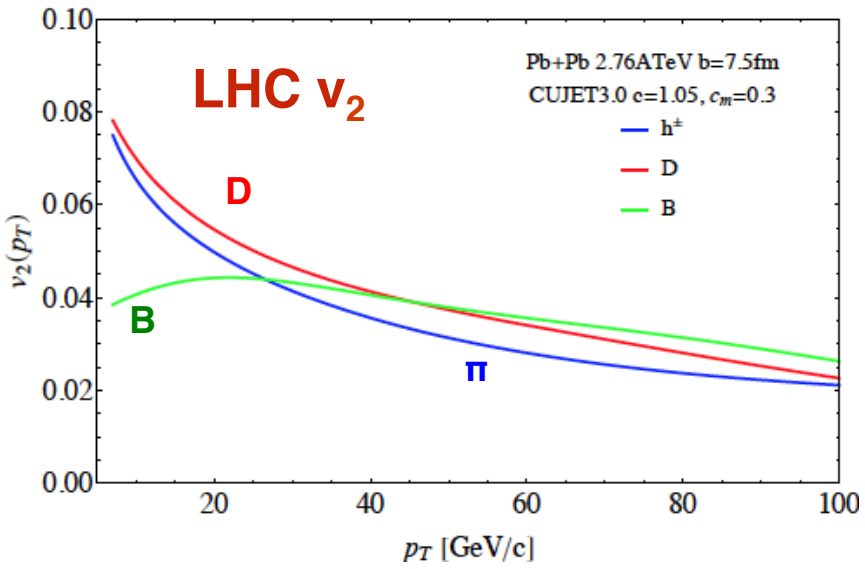

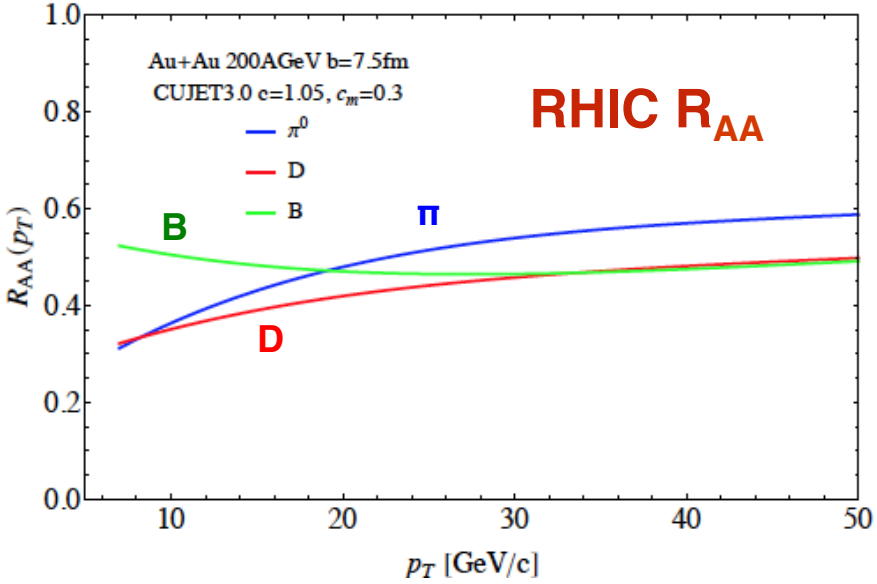

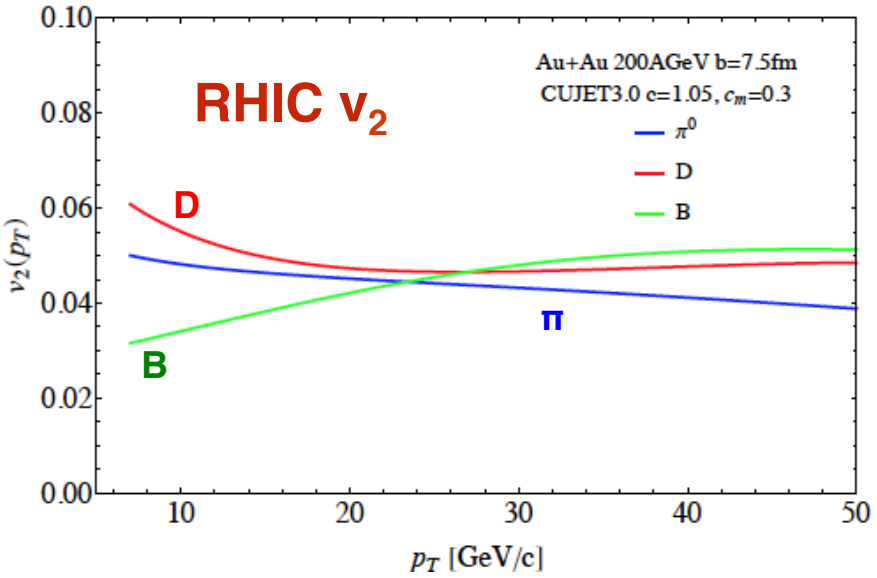

CUJET3.0: qhat(E,T) for quark jets in sQGMP

Liu et al. PRL 2006
$\hat{q} \approx 26.69\sqrt{\lambda/4\pi}T^3$

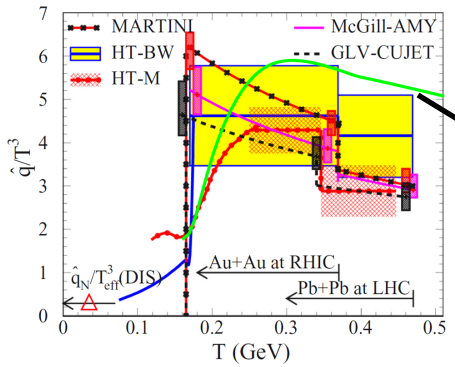

JET Collaboration, PRC 2014

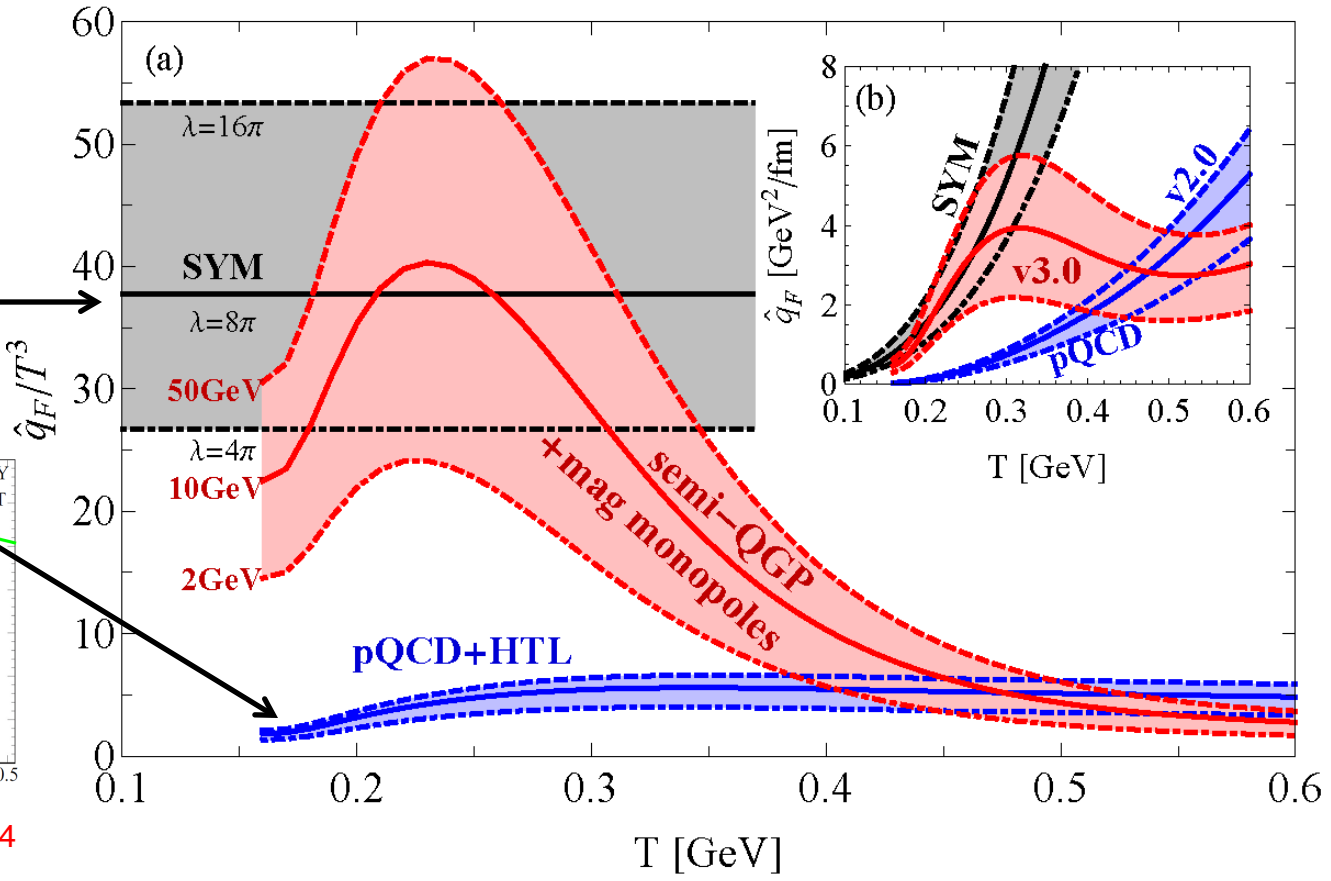

$$\hat{q}_F = \int_0^{6ET} dq^2 \frac{2\pi q^2}{(q^2+f_E^2\mu^2)(q^2+f_M^2\mu^2)}\rho(T) \times \left[(C_{qq}f_q + C_{qg}f_g)\alpha_s^2(q^2) + C_{qm}(1-f_q-f_g)\right]$$

$$f_q = c_q L(T),\ f_g = c_g L(T)^2$$
$$\rho(T) \sim p(T)/T$$ p(T) from s95p-PCE EOS

- CUJET3.0 solution exhibits a “volcano” interpolation of qhat/T^3 between strong “AdS-like” sQGP at T=200-350MeV to more transparent “HTL-like” QGP for T>400MeV

pQCD jet quenching + sQGMP: η/s(T)

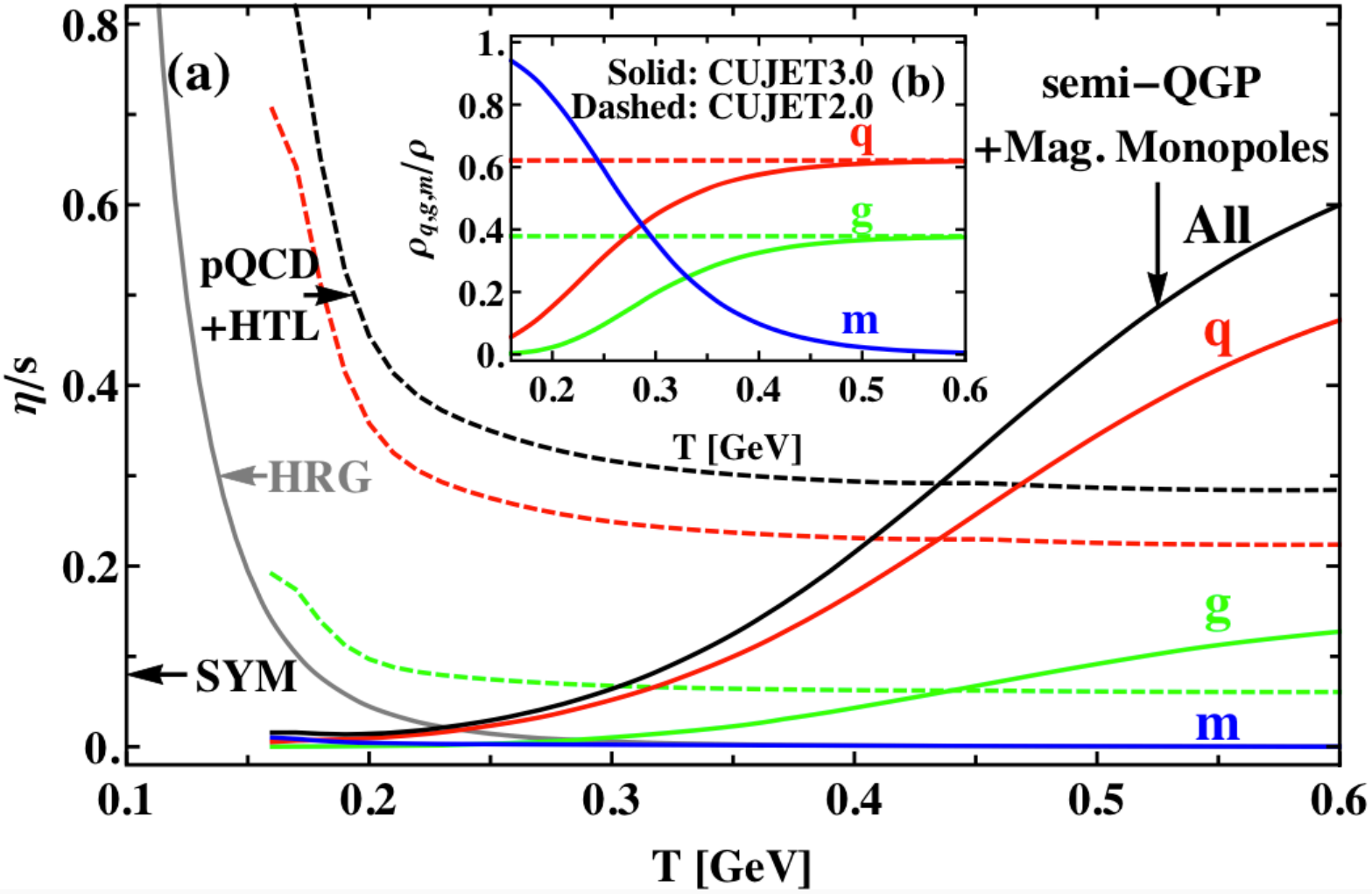

- CUJET3.0 provides a quantitative connection between the jet transport properties controlling the hard jet quenching observables and the bulk viscous transport properties controlling the soft "perfect fluidity" of QGP observed at RHIC and LHC.

Near-Tc properties of sQGMP are special!

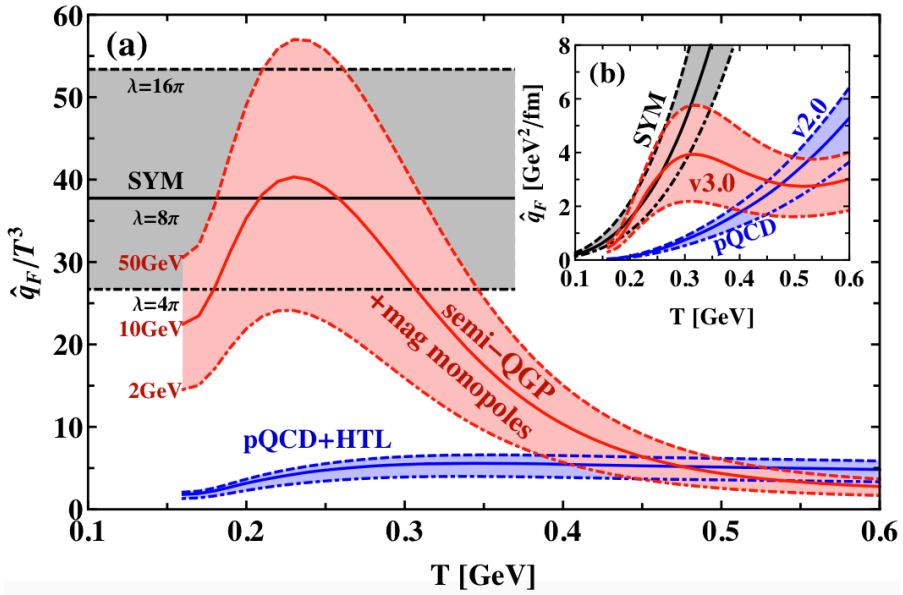

Jet transport coefficient qhat/T^3 computed from CUJET3.0 shows a prominent peak near Tc!

Shear viscosity, η/s, computed from CUJET3.0 shows a clear minimum near Tc and a rapid rise at high T!

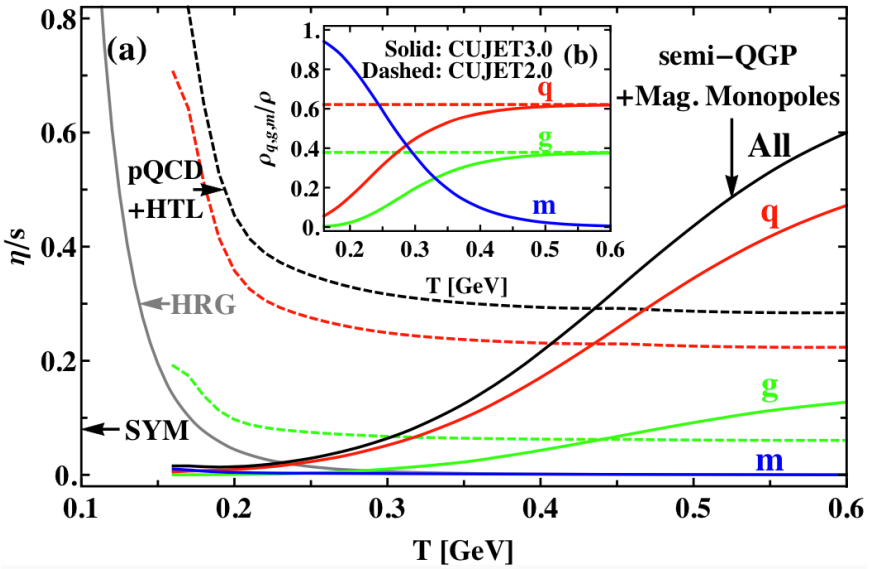

CUJET3.0 = [pQCD] + [semi-QGP] + [magnetic monopoles] bridges the "soft" bulk perfect fluidity and the "hard" jet quenching (η/s~T^3/qhat)

BES@RHIC and LHC are both essential to constrain and map out the strongly non-conformal QCD confinement transition physics

Summary

- CUJET2.0 = [rcDGLV+Elastic] + [2+1D Viscous Hydro] solves the "heavy quark energy loss puzzle" and explains the "surprising transparency of QGP at LHC"

- Combining the pQCD jet quenching kernal and the microscopic semi-Quark-Gluon Monopole Plasma (sQGMP) model, CUJET3.0 describes $(R_{AA}+v_2) \times$ (pion+D+B) $\times$ (RHIC+LHC) simultaneously
  - qhat from CUJET3.0 smoothly bridges the N=4 SYM limit near Tc and the HTL pQCD limit at high T
  - eta/s from CUJET3.0 approaches the perfect fluidity ~0.1 near Tc, and rises rapidly at high T

Thank you!

Backup

Color confinement: Dual Superconductivity

- Dual superconductivity is a promising mechanism for quark confinement. [Y.Nambu (1974). G.'t Hooft, (1975). S.Mandelstam, (1976) A.M. Polyakov (1975)]

superconductor

- Condensation of electric charges (Cooper pairs)
- Meissner effect: Abrikosov string (magnetic flux tube) connecting monopole and anti-monopole
- Linear potential between monopoles

dual superconductor

- Condensation of magnetic monopoles
- Dual Meissner effect: formation of a hadron string (chromo-electric flux tube) connecting quark and antiquark
- Linear potential between quarks

Akihiro, Shibata, Trento 2013

Kondo, Kato, Shibata, Shinohara, arXiv:1409.1599

(D)GLV Opacity Expansion

$$x\frac{dN_g^n}{dxd^2\mathbf{k}} = \frac{C_R\alpha_s}{\pi^2}\frac{1}{n!}\left(\frac{L}{\lambda_g}\right)^n \int\prod_{i=1}^{n}\left(d^2\mathbf{q}_i\left(|\bar{v}_i(\mathbf{q}_i)|^2-\delta^2(\mathbf{q}_i)\right)\right)$$

$$\times\ -2\,\mathbf{C}_{(1\cdots n)}\cdot\sum_{m=1}^{n}\mathbf{B}_{(m+1\cdots n)(m\cdots n)}$$

$$\times\left(\cos\left(\sum_{k=2}^{m}\Omega_{(k\cdots n)}\Delta z_k\right)-\cos\left(\sum_{k=1}^{m}\Omega_{(k\cdots n)}\Delta z_k\right)\right)$$

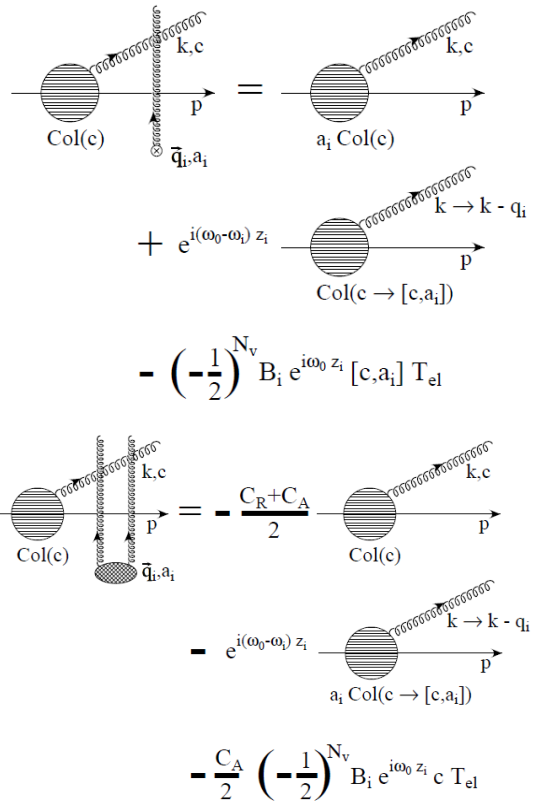

$$\mathbf{C}_{(1\cdots n)} = \frac{\mathbf{k}-\mathbf{q}_1-\cdots-\mathbf{q}_n}{(\mathbf{k}-\mathbf{q}_1-\cdots-\mathbf{q}_n)^2+\chi^2}$$

$$\mathbf{H} = \frac{\mathbf{k}}{\mathbf{k}^2+\chi^2}$$

$$\mathbf{B}_{(i)} = \mathbf{H}-\mathbf{C}_{(i)}$$

$$\mathbf{B}_{(1\cdots m)(1\cdots n)} = \mathbf{C}_{(1\cdots m)}-\mathbf{C}_{(1\cdots n)}$$

$$\Omega_{m\cdots n} = \frac{(\mathbf{k}-\mathbf{q}_m-\cdots-\mathbf{q}_n)^2+\chi^2}{2xE}$$

(Gyulassy, Levai, Vitev, Djordjevic)

$$\chi^2 = M^2x^2 + m_g^2(1-x) \quad m_g = \mu/\sqrt{2}\ ,\ \mu = gT\sqrt{N_c/3+N_f/6}$$

$$|\bar{v}_i(\mathbf{q}_i)|^2 = \frac{{\mu_i}^2}{\pi(\mathbf{q}_i^2+{\mu_i}^2)^2}$$ (Gyulassy-Wang, 1996)

Convergence of the DGLV opacity series

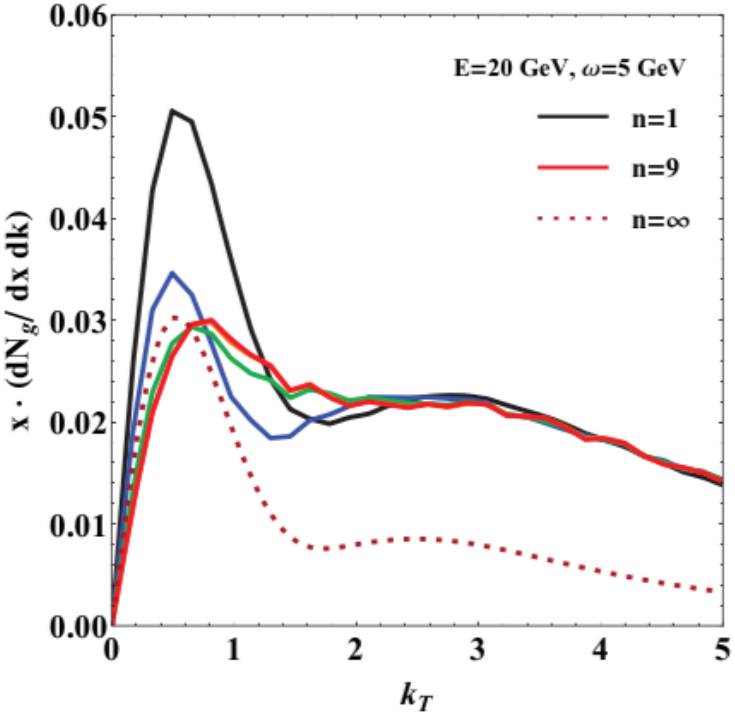

Figure 15. Radiated gluon transverse momentum distribution for a heavy quark jet with energy $E = 20\,\mathrm{GeV}$ traversing a brick plasma of size $L = 5\,\mathrm{fm}$ emitting a gluon with energy $\omega = 5\,\mathrm{GeV}$. The mass of the quark $M = 4.75\,\mathrm{GeV}$. The DGLV opacity series calculated up to n=1 (black), 3 (blue), 5 (green), 7 (orange), 9 (red) are shown in the figure. The opacity expansion computed up to ninth order is shown to converge to the ASW multiple soft scattering limit (maroon, dashed) for small $k_\perp \lesssim \hat{q}L \approx 1\,\mathrm{GeV}$. At large $k_\perp$, differs from the ASW limit, DGLV has a robust Laudau tail. Other parameters used in the simulation are: $\lambda = 1.16\,\mathrm{fm}$, $\mu = 0.5\,\mathrm{GeV}$, $m_g = 0.356\,\mathrm{GeV}$, $T = 0.258\,\mathrm{GeV}$, $n_f = 0$, $\alpha_s = 0.3$.

JX, Buzzatti, Gyulassy, JHEP 1408, 063 (2014)

Review the kernel of CUJET1.0

Radiative: dynamical DGLV

$$x_E\frac{dN_g^{n=1}}{dx_E}(\mathbf{x}_0,\phi)=\frac{18C_R\alpha_s}{\pi^2}\frac{4+n_f}{16+9n_f}\int d\tau\,\rho(\mathbf{z})\int d^2\mathbf{k}\int d^2\mathbf{q}\;\alpha_s^2|\tilde{v}(\mathbf{q},\mathbf{z})|^2$$
$$\times\;\frac{-2(\mathbf{k}-\mathbf{q})}{(\mathbf{k}-\mathbf{q})^2+\chi^2(\mathbf{z})}\left(\frac{\mathbf{k}}{\mathbf{k}^2+\chi^2(\mathbf{z})}-\frac{(\mathbf{k}-\mathbf{q})}{(\mathbf{k}-\mathbf{q})^2+\chi^2(\mathbf{z})}\right)$$
$$\times\;\left(1-\cos\left(\frac{(\mathbf{k}-\mathbf{q})^2+\chi^2(\mathbf{z})}{2x_+E}\tau\right)\right)$$
$$\times\;\left(\frac{x_E}{x_+}\right)J(x_+(x_E))$$

$$|\tilde{v}(\mathbf{q},\mathbf{z})|^2=\frac{f_E^2-f_M^2}{(\mathbf{q}^2+f_E^2\mu^2(\mathbf{z}))(\mathbf{q}^2+f_M^2\mu^2(\mathbf{z}))}$$

$$\chi^2(\mathbf{z})=M^2x_+^2+m_g^2(\mathbf{z})(1-x_+),\; m_g(\mathbf{z})=\mu(\mathbf{z})/\sqrt{2}$$

$$\mu^2(\mathbf{z})=g^2f_E^2T(\mathbf{z})^2\,(1+n_f/6)=4\pi\alpha_sf_E^2T(\mathbf{z})^2\,(1+n_f/6)$$

$$0\le k_\perp\le x_EE\;,\;0\le q_\perp\le \mathrm{Min}\{k_\perp,\sqrt{4ET(\mathbf{z})}\}$$

$$x_+(x_E)=\frac{1}{2}x_E\left(1+\sqrt{1-\left(\frac{k_\perp}{x_EE}\right)^2}\right)\qquad J(x_+(x_E))\equiv\frac{dx_+}{dx_E}=\frac{1}{2}\left(1+\left(1-\left(\frac{k_\perp}{x_EE}\right)^2\right)^{-1}\right)$$

Elastic: Thoma-Gyulassy (TG)

$$\frac{dE(\mathbf{z})}{d\tau}=-C_R\pi\alpha_s^2T(\mathbf{z})^2\left(1+\frac{n_f}{6}\right)\log\left(\frac{4T(\mathbf{z})\sqrt{E(\mathbf{z})^2-M^2}}{\left(E(\mathbf{z})-\sqrt{E(\mathbf{z})^2-M^2}+4T(\mathbf{z})\right)\mu(\mathbf{z})}\right)$$

CUJET3.0: HF Decay Electron RAA & v2

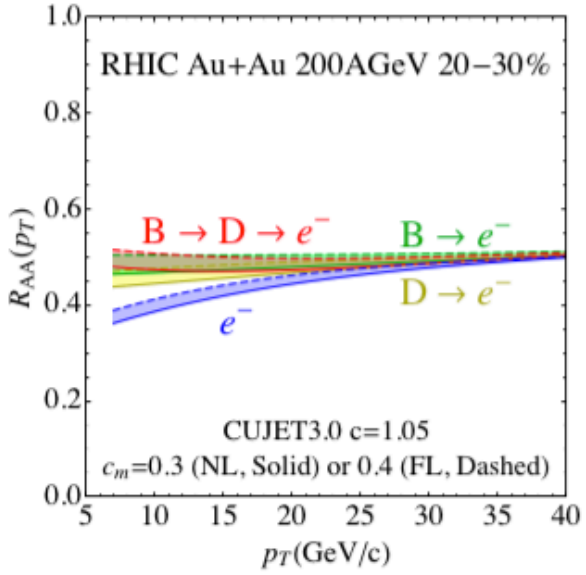

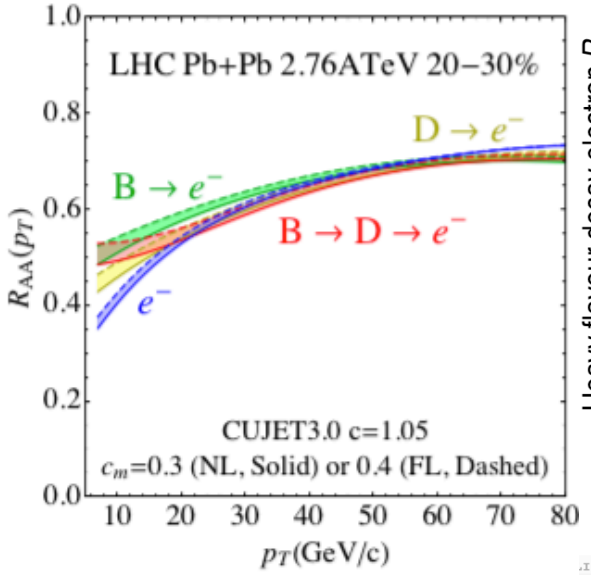

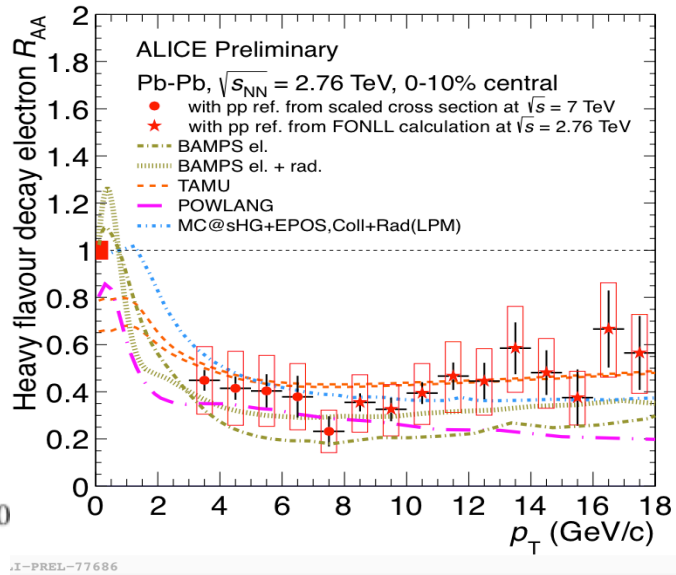

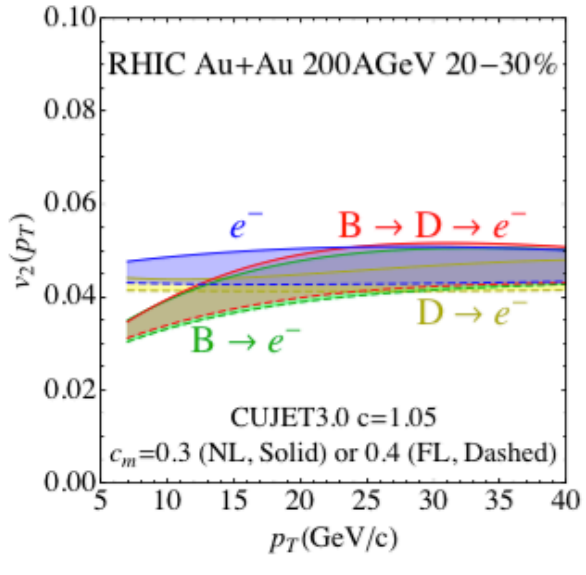

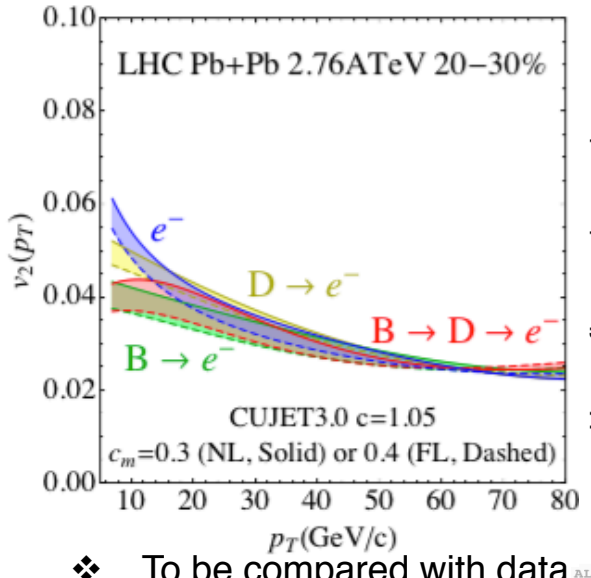

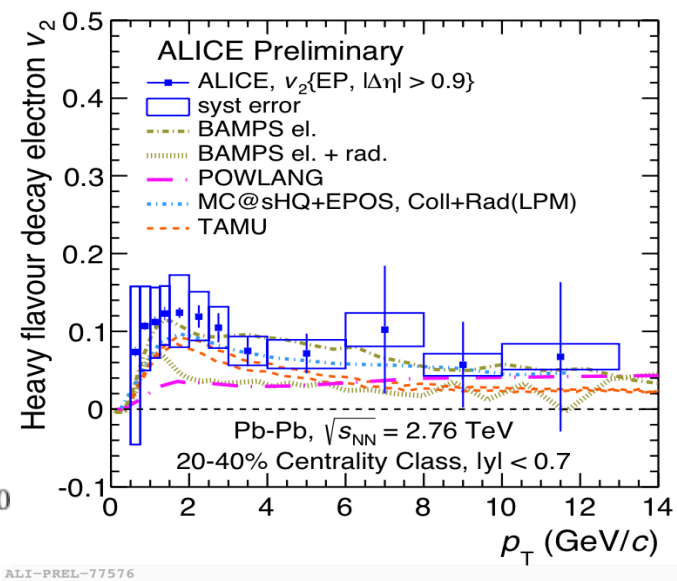

- To be compared with data

More about the multi-scale running coupling

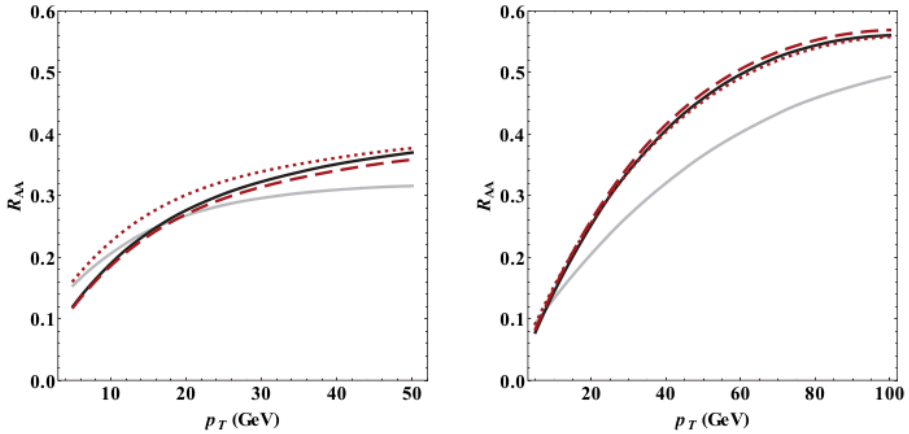

Figure 1. Fixed and running coupling pion R_{AA} results are compared side to side at RHIC (*left*) and LHC (*right*) in CUJET with Glauber static transverse plus Bjorken longitudinal expanding background. The gray opaque curves use a fixed coupling with $\alpha_s = 0.3$, while the black curves use a running coupling with $\alpha_{\max} = 0.4$. The difference is notable, especially in the higher energy range available at the LHC, while RHIC results are left almost unchanged. The sensitivity to the variation of running scales Q_i (cf. eq. (2.1) and following) is measured by the red curves: on one side we decrease the value of all scales Q_i by 50% and lower $\alpha_{\max}$ to 0.3 (red dashed), on the other we increase all scales Q_i by 25% and increase at the same time $\alpha_{\max}$ to 0.6 (red dotted). $\alpha_{\max}$ is constrained to fit $R_{AA}^{\pi,LHC}(p_T \approx 30\ \text{GeV}) = 0.35$.

❖ Uncertainties in running scales

❖ Which running scale dominates?

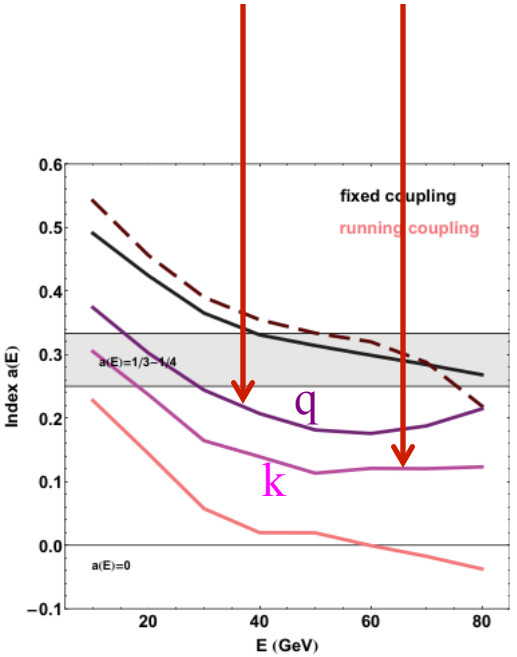

Figure 2. Energy loss index $a(E)$ (cf. eq. (2.9)) for different assumptions of the running coupling in CUJET: fixed effective $\alpha_s = 0.3$ (black), only thermal coupling running (dashed red), only $\alpha_s^2(\mathbf{q}^2)$ running (purple), only $\alpha_s^2(\mathbf{k}^2/(x(1-x)))$ running (magenta), all couplings running (pink). The saturated $\alpha_{\max}$ value is chosen to be equal to 0.4, which corresponds to approximately $Q_0 \sim 1\,\text{GeV}$. The plot shows the energy loss of a light quark ($M = 0.2\,\text{GeV}$) traveling from the origin of the transverse plane and through a gluonic plasma ($n_f = 0$) of size $L = 5\,\text{fm}$, whose density profile is generated from Glauber model and resembles the medium created in a Pb+Pb $\sqrt{s_{NN}} = 2.76\,\text{TeV}$ $b = 0\,\text{fm}$ collision.

More on the Polyakov Loop

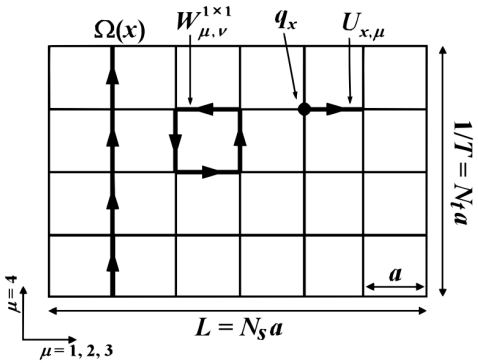

$$U_{x,\mu} = \mathcal{P}\exp\left[ig\int_x^{x+\hat{\mu}} dx_\mu A_\mu(x)\right]$$

$$W^{1\times1}_{\mu\nu}(x) \equiv U_{x,\mu}U_{x+\hat{\mu},\nu}U^\dagger_{x+\hat{\nu},\mu}U^\dagger_{x,\nu}.$$

$$L(\mathbf{x}) = \frac{1}{N_c}\mathrm{tr}\mathcal{P}\exp\left[ig\int_0^{1/T} A_4(\tau,\mathbf{x})d\tau\right] \equiv \frac{1}{N_c}\mathrm{tr}\Omega(\mathbf{x})$$

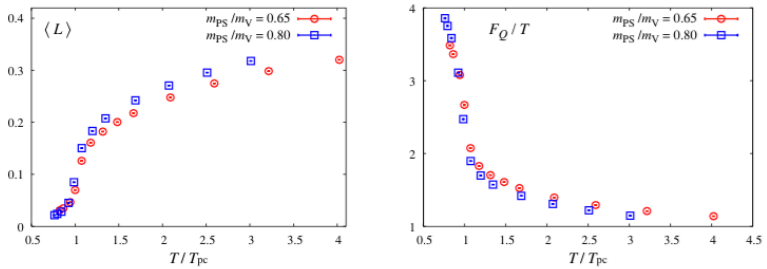

Figure 2.5: Polyakov loop (left) and single-quark free energy (right) on lines of constant physics at $m_{PS}/m_V = 0.65$ (circle) and 0.80 (square) as a function of temperature.

shows the free energy of a single quark defined as

$$\frac{F_Q}{T} = -\ln\langle L\rangle. \tag{2.62}$$

We find that the free energy for smaller quark mass is smaller below T_{pc}, whereas it is larger above T_{pc} than that for larger quark mass. This implies that the anti-screening (screening) properties in the confinement (deconfinement) phase becomes strong when the quark mass is reduced.

The physical meanings of the Polyakov loop can be seen as follows. Consider the equation of motion for the heavy quark field which is written as $e^{-m_Q\tau}\psi$ (upper component of the Dirac spinor). The static Dirac equation for ψ is given as,

$$\left(i\frac{\partial}{\partial\tau} + gA_4(\tau,\mathbf{x})\right)\psi(\tau,\mathbf{x}) = 0. \tag{2.58}$$

The solution is

$$\psi^a(\tau,\mathbf{x}) = \Omega^{ab}(\mathbf{x})\,\psi^b(0,\mathbf{x}), \tag{2.59}$$

where color indices are written explicitly. When the heavy (static) quark is placed at a spatial point $\mathbf{x}$, the partition function (Z_Q) for the single quark can be written by the total Hamiltonian H_Q as:

$$\begin{aligned} Z_Q/Z &= e^{-(F_Q(T,V)-F(T,V))/T} \\ &= \frac{1}{Z}\frac{1}{N_c}\sum_{a=1}^{N_c}\sum_n \langle n|\psi^a(0,\mathbf{x})e^{-H_Q/T}\psi^{\dagger a}(0,\mathbf{x})|n\rangle \\ &= \frac{1}{Z}\frac{1}{N_c}\sum_{a=1}^{N_c}\sum_n \langle n|e^{-H_Q/T}\psi^a(1/T,\mathbf{x})\psi^{\dagger a}(0,\mathbf{x})|n\rangle \\ &= \frac{1}{Z}\frac{1}{N_c}\mathrm{tr}\left[e^{-H/T}\mathrm{tr}\Omega(\mathbf{x})\right] = \langle L(\mathbf{x})\rangle, \end{aligned} \tag{2.60}$$

where F_Q (F) is the free energy with (without) the heavy quark. In the $N_f = 0$ case, the free energy of a single quark can strictly distinguish the confinement phase and the deconfinement phase. Although the Polyakov loop is no longer the order parameter for confinement-deconfinement transition in the case with dynamical quarks, we can utilize the $\langle L\rangle$ as an indicator to separate the cold and hot phases in the parameter space (see Fig. 2.2). The nu-

as the Polyakov loop averaged over all thermal states and spatial points,

$$\langle L\rangle = \frac{1}{Z}\frac{1}{N_s^3}\sum_{\mathbf{x}}\mathrm{Tr}\left[e^{-H/T}L(\mathbf{x})\right]. \tag{2.61}$$

The Polyakov loop has finite values even below T_{pc} because a single heavy quark can exist in the confinement phase due to the dynamical screening from the light quarks. Figure 2.5(right)

Adapted from Maezawa 2007

CUJET3.0 = CUJET2.0 + semi-QGP + mag. monopoles

$$\frac{dE}{dx} \propto ... \int_{q^2} \left[\frac{n_e \left(\alpha_s(q^2)\alpha_s(q^2)\right) f_E^2}{q^2(q^2+f_E^2\mu^2)} + \frac{n_m \left(\alpha_s^e(q^2)\alpha^m(q^2)\right) f_M^2}{q^2(q^2+f_M^2\mu^2)} \right] ...$$

$$\frac{dE}{dx} \propto ... \int_{q^2} \frac{n_e\, \alpha_s^2(q^2)\, f_E^2}{q^2(q^2+f_E^2\mu^2)} ...$$

$$\frac{dE}{dx} \propto ... \int_{q^2} \frac{n_T}{(q^2+f_E^2\mu^2)(q^2+f_M^2\mu^2)} \times \kappa(q^2,T)$$

$$\kappa(q^2,T) \equiv \alpha_s^2(q^2)\,\chi_T \left(f_E^2 + \frac{f_E^2 f_M^2 \mu^2}{q^2}\right) + (1-\chi_T)\left(f_M^2 + \frac{f_E^2 f_M^2 \mu^2}{q^2}\right)$$

$$\chi_T = c_q\, L + c_g\, L^2 \qquad L(\mathbf{x}) = \frac{1}{N_c}\mathrm{tr}\mathcal{P}\exp\left[ig\int_0^{1/T} A_4(\tau,\mathbf{x})d\tau\right]$$

$$f_E = \sqrt{\chi_T}$$

$$f_M = C_m\, g_T$$

$$x_E \frac{dN_g^{n=1}}{dx_E} = \frac{18C_R}{\pi^2}\frac{4+N_f}{16+9N_f}\int d\tau\, n(\mathbf{z})\Gamma(\mathbf{z}) \int d^2k$$
$$\times\, \alpha_s\left(\frac{\mathbf{k}^2}{x_+(1-x_+)}\right) \int d^2q \frac{\alpha_s^2(\mathbf{q}^2)}{\mu^2(\mathbf{z})} \frac{f_E^2\mu^2(\mathbf{z})}{\mathbf{q}^2(\mathbf{q}^2+f_E^2\mu^2(\mathbf{z}))}$$
$$\times \frac{-2(\mathbf{k}-\mathbf{q})}{(\mathbf{k}-\mathbf{q})^2+\chi^2(\mathbf{z})}\left[\frac{\mathbf{k}}{\mathbf{k}^2+\chi^2(\mathbf{z})} - \frac{(\mathbf{k}-\mathbf{q})}{(\mathbf{k}-\mathbf{q})^2+\chi^2(\mathbf{z})}\right]$$
$$\times \left[1-\cos\left(\frac{(\mathbf{k}-\mathbf{q})^2+\chi^2(\mathbf{z})}{2x_+E}\tau\right)\right]\left(\frac{x_E}{x_+}\right)\left|\frac{dx_+}{dx_E}\right| \qquad (1)$$

$$\Gamma(\mathbf{z}) = u_f^\mu n_\mu \qquad n = (1,\vec{\beta}_{jet})$$

Liu et al. 07'; Baier et al. 07' $\qquad u_f^\mu = \gamma_f(1,\vec{\beta}_f)$

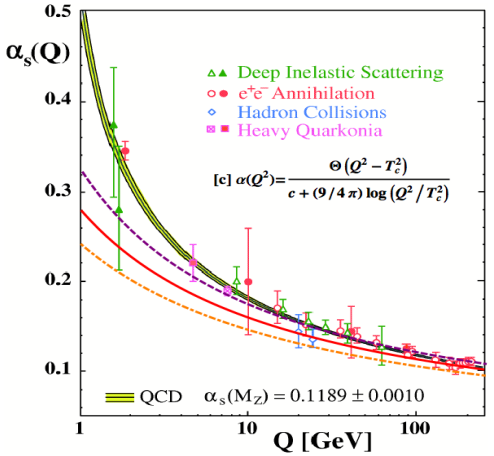

$$\alpha_s^2(q^2) \approx [1/[c+(9/2\pi)Log(q/\Lambda)]]^2$$

Pressure/Entropy Counting & eta/s

- The eta/s in kinetic theory
- Extra factors come from quantum statistics which differ slightly from the Stefan-Boltzmann
- Different counting schemes bring theoretical uncertainties

$$\frac{\eta}{s} = \frac{18}{5}\frac{T^3}{s(T)}\sum_a \frac{d_a(T)}{\sum_b d_b(T) F_{ab}(T)}$$

$$a, b = q, g, m$$

$$d_q = c_q \cdot L(T)\ (PR)\ or\ c_q \cdot L(T)/N_s\ (SR)$$

$$d_g = c_g \cdot L^2(T)\ (PR)\ or\ c_g \cdot L^2(T)/N_s\ (SR)$$

$$d_m = 1 - d_q - d_g$$

$$F_{ab}(T) = \int_0^{9T^2} dq^2 \frac{2\pi q^2 C_{ab}\alpha_a\alpha_b}{(q^2 + f_E^2\mu^2)(q^2 + f_M^2\mu^2)}$$

$$\alpha_q = \alpha_g = \alpha_E\ ,\ \alpha_m = 1/\alpha_E$$

$$C_{qq} = 4/9$$

$$C_{qg} = C_{gq} = C_{qm} = C_{mq} = 1$$

$$C_{gg} = C_{mm} = 9/4$$

$$\begin{aligned}
\rho(\mathbf{x}) &= \sum \frac{\zeta(3)}{\pi^2} g_i \eta_i T^3(\mathbf{x}) \\
\epsilon(\mathbf{x}) &= \sum \frac{\pi^2}{30} g_i \eta_i' T^4(\mathbf{x}) \\
p(\mathbf{x}) &= \epsilon(\mathbf{x})/3 \\
s(\mathbf{x}) &= \frac{p(\mathbf{x}) + \epsilon(\mathbf{x})}{T} \approx \kappa\rho(\mathbf{x})
\end{aligned}$$

Fast Liberation Scheme (FL)

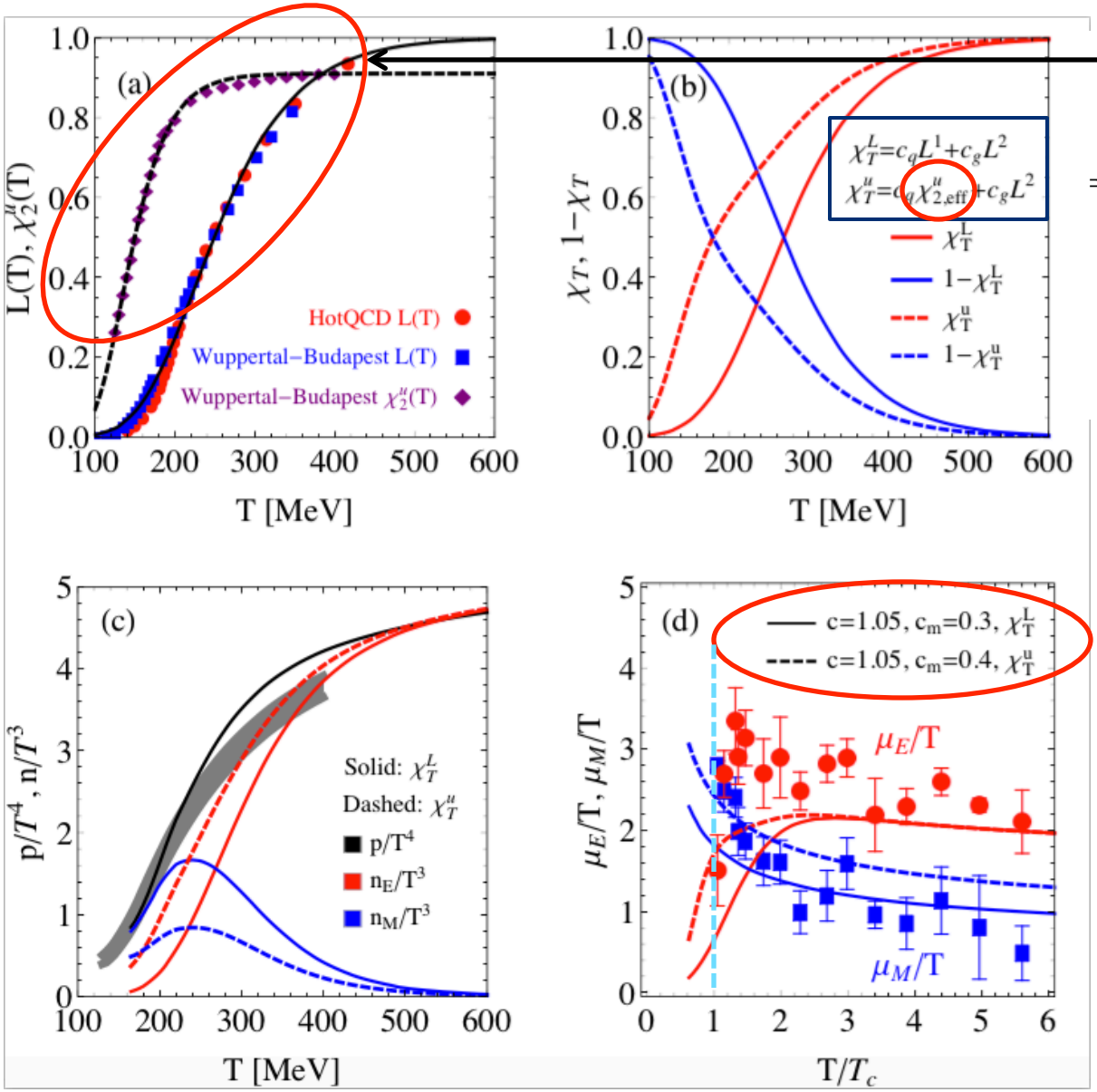

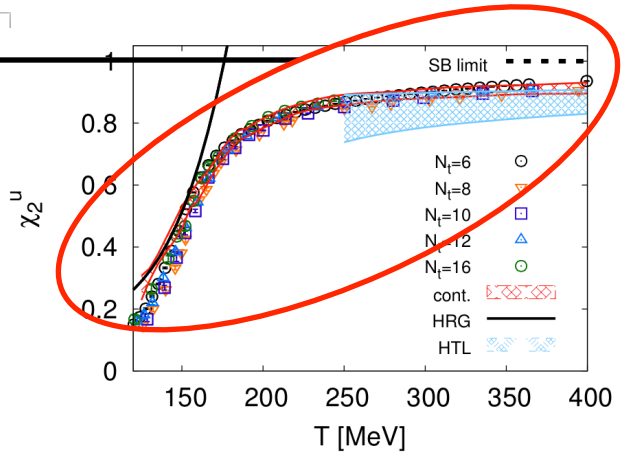

Wuppertal-Budapest JHEP 1201 (2012) 138

- Fast Quark Liberation: Fit to lattice QCD u quark number susceptibility
- Note the shift of E&M fractions and screening masses near Tc

$$\frac{p}{T^4}=\frac{1}{VT^3}\ln Z(V,T,\mu_B,\mu_S,\mu_Q)$$

$$\chi_{lmn}^{BSQ}=\frac{\partial^{l+m+n}p/T^4}{\partial(\mu_B/T)^l\partial(\mu_S/T)^m\partial(\mu_Q/T)^n}.$$

$$\chi_2^X=\frac{1}{VT^3}\langle N_X^2\rangle$$

CUJET3.0: RAA & v2 at RHIC & LHC in FL

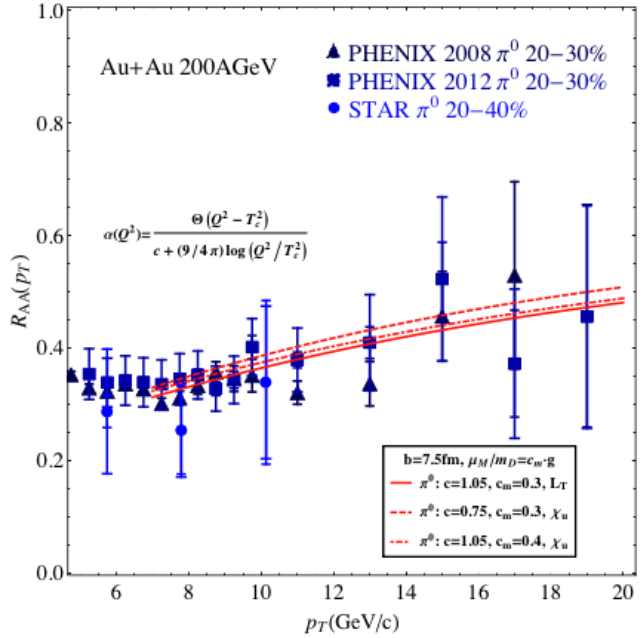

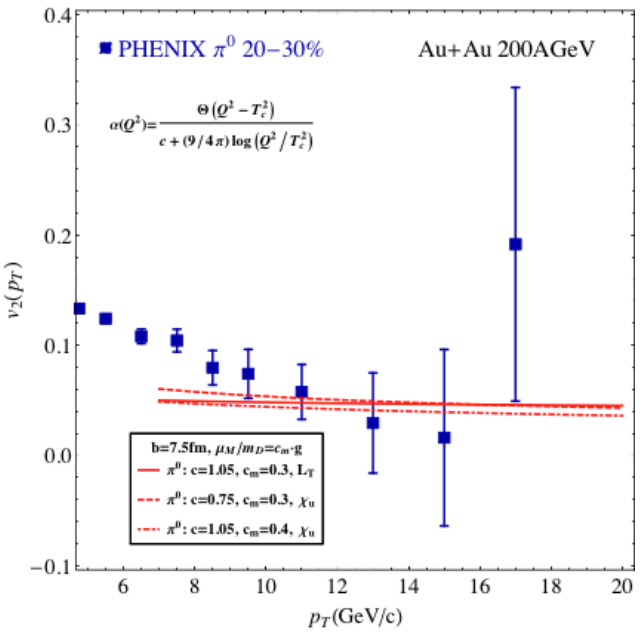

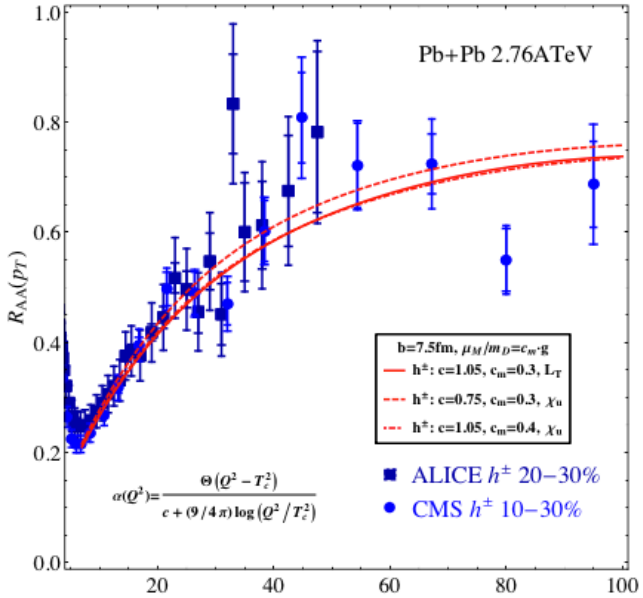

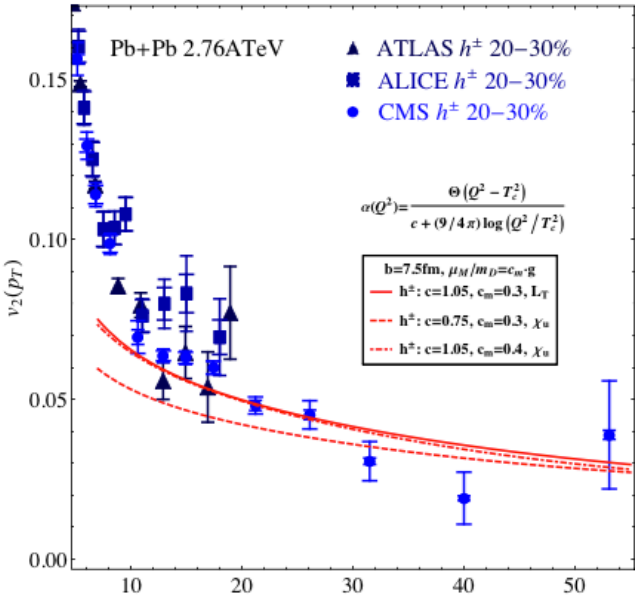

CUJET3.0: RAA & v2 at RHIC & LHC in FL

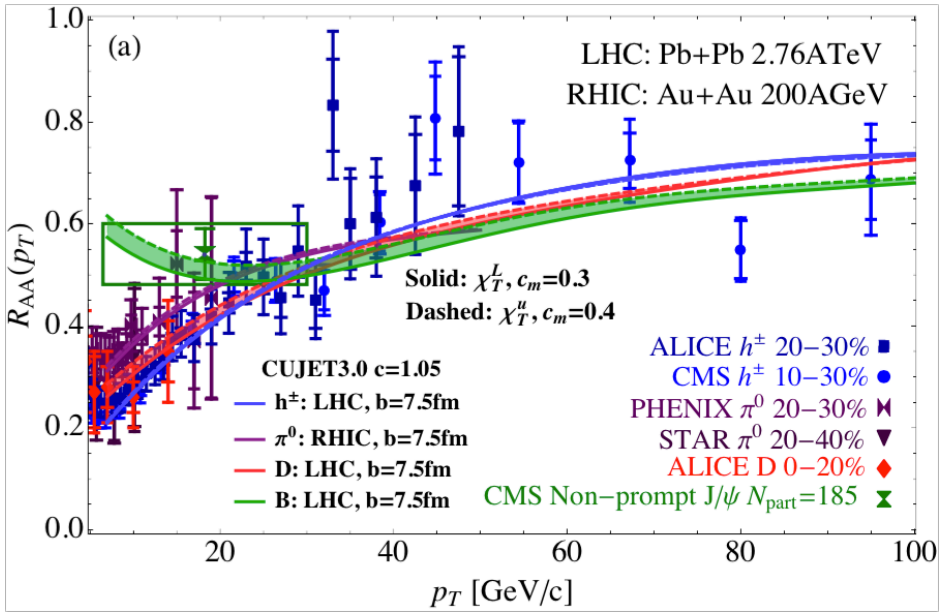

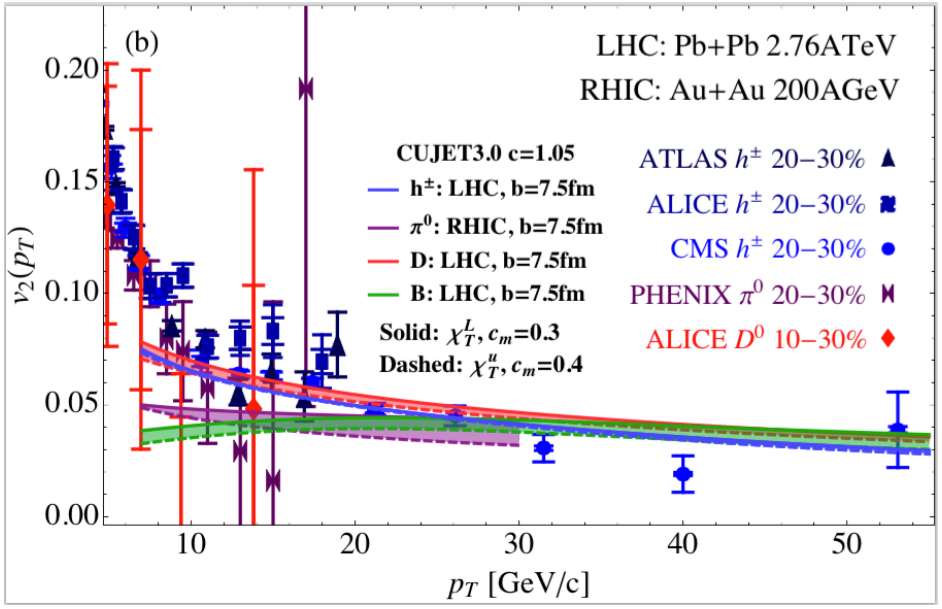

- In the fast liberation scheme, the CUJET3.0 model with $(c,c_m)=(1.05,0.4)$ fits both R_{AA} and v_2 at both RHIC and LHC

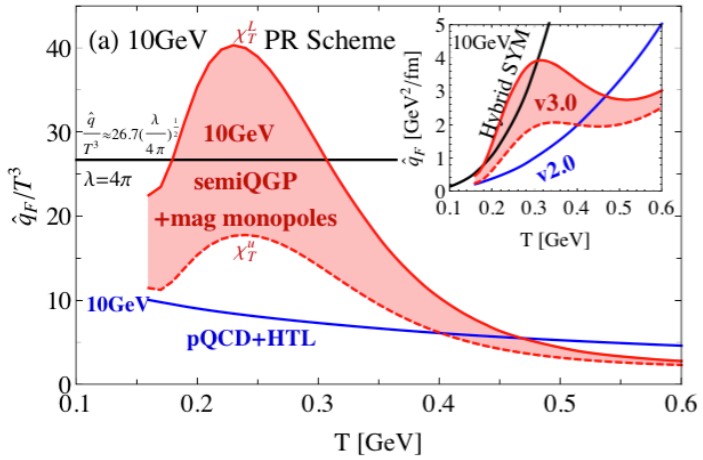

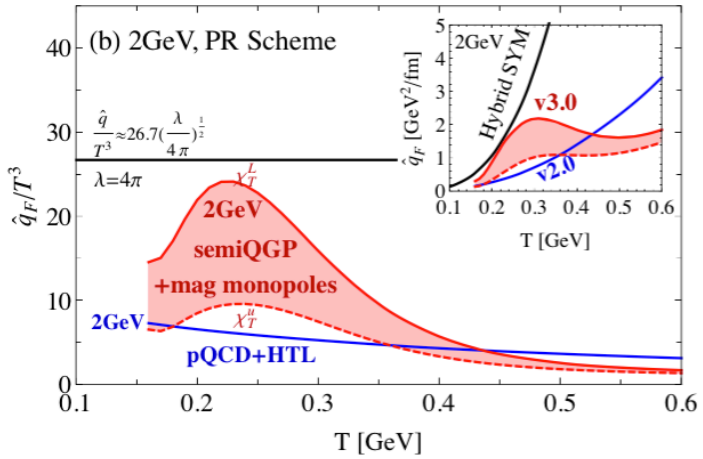

CUJET3.0: eta/s in the fast liberation scheme

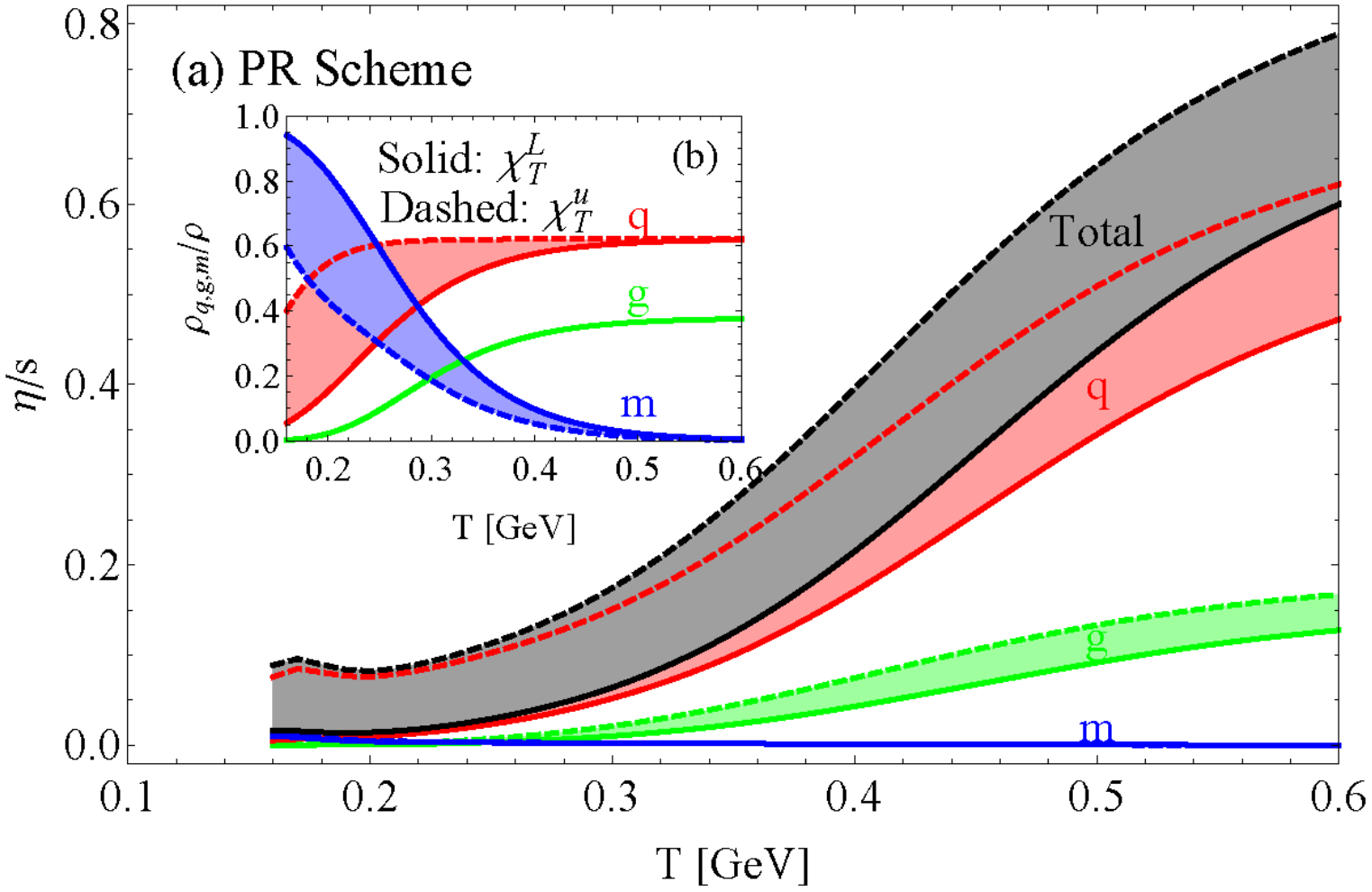

- Fast liberation gives a better eta/s near Tc

Relativistic corrections to jet quenching from transverse flow

$$\Gamma(\mathbf{z}) = u_f^\mu n_\mu \quad n = (1, \vec{\beta}_{jet}) \quad u_f^\mu = \gamma_f (1, \vec{\beta}_f)$$ Liu et al. 07'; Baier et al. 07'

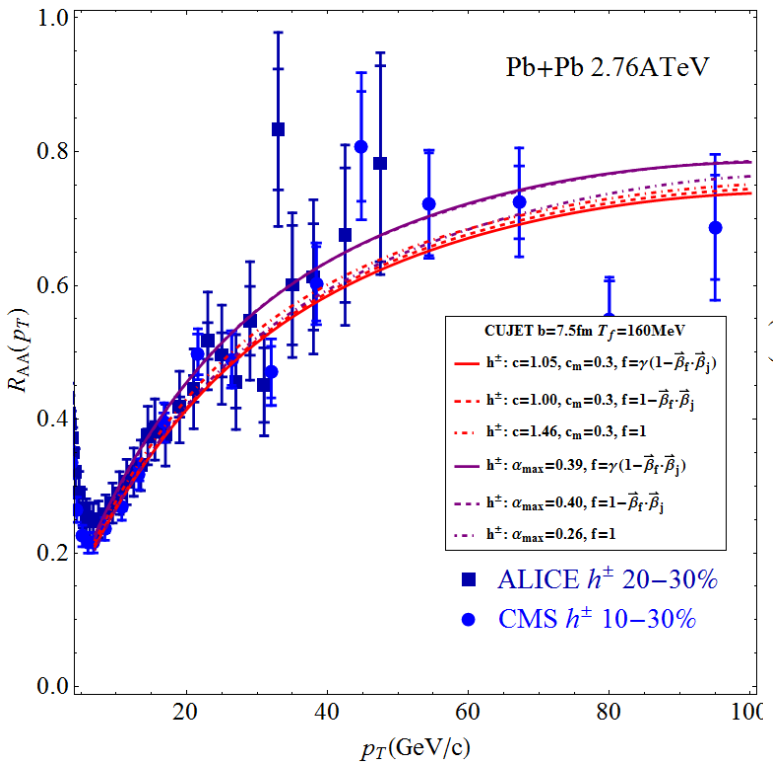

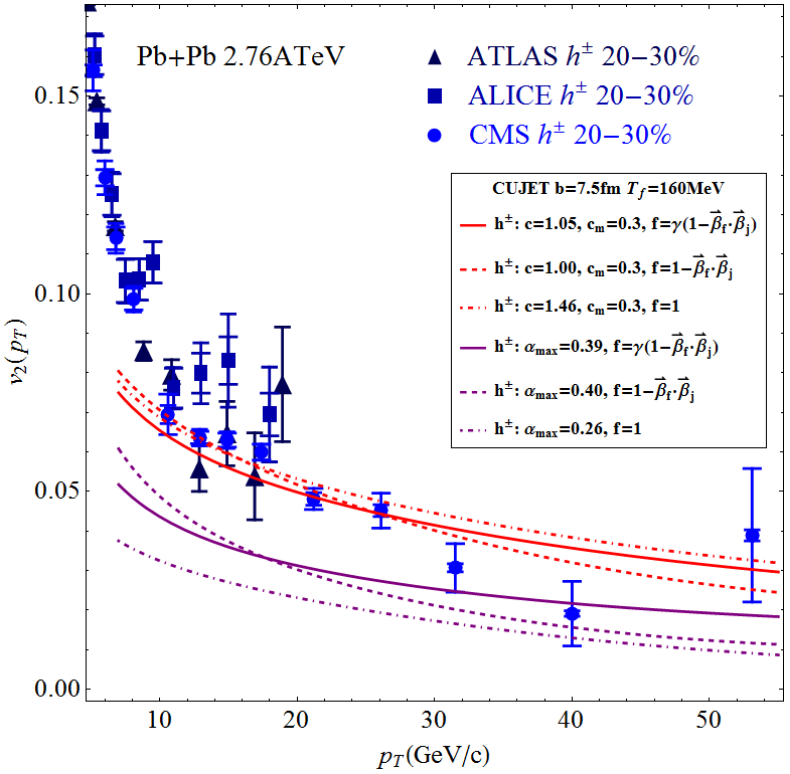

- Both RAA and v2 are surprisingly insensitive to the form of the relativistic flow corrections in both CUJET2.0 (pQCD+HTL) and CUJET3.0 (semi-QGP + magnetic monopoles)

CUJETv3.0 vs v2.0: the path length dependence of energy loss

log(ΔE/E) vs log(L)

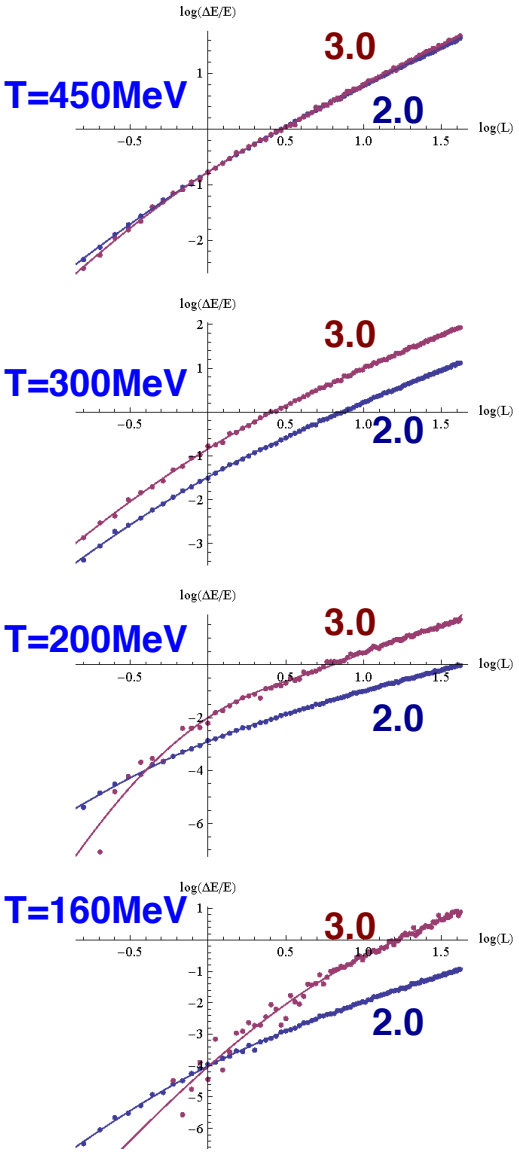

n(L) vs L; dE/dL~L^n

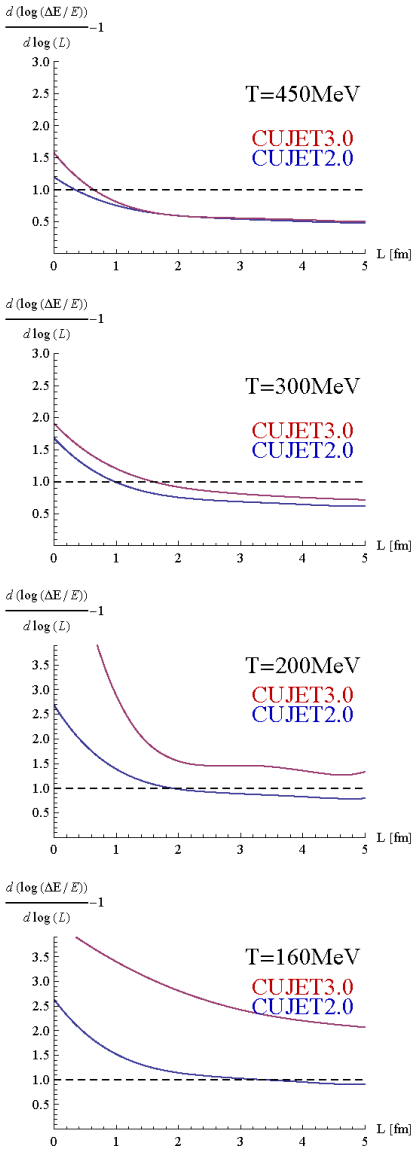

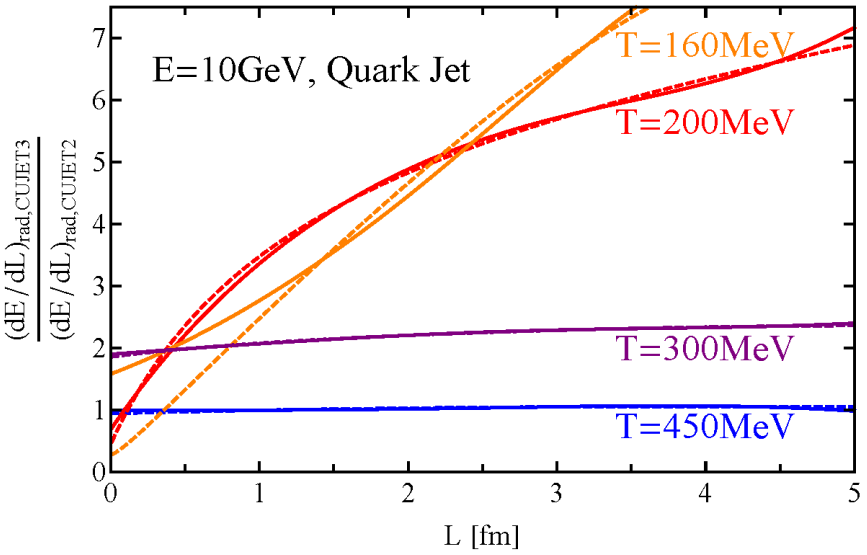

- At high T, v2.0 and v3.0 are similar, both bearing dE/dL~L^n with n~0.5, stronger than linear and weaker than quadratic
- At intermediate T, v2.0 and v3.0 are approximately similar with n~1
- At near-Tc temperatures, CUJET v2.0 is roughly a quadratic dependence and v3.0 is about CUBIC!
  - At small distances, the energy loss of v3.0 is smaller than v2.0=pQCD+HTL